9
Signaling at the Nerve-Muscle Synapse: Directly Gated Transmission

COMMUNICATION BETWEEN NEURONS in the brain relies mainly on chemical synapses. Much of our present understanding of the function of these synapses is based on studies of synaptic transmission at the nerve-muscle synapse, the junction between a motor neuron and a skeletal muscle fiber. This is the site where synaptic transmission was first studied and remains best understood. Moreover, the nerve-muscle synapse is the site of a number of inherited and acquired neurological diseases. Therefore, before we examine the complexities of synapses in the central nervous system, we will examine the basic features of chemical synaptic transmission at the nerve-muscle synapse.

The nerve-muscle synapse is an ideal site for studying chemical signaling because it is relatively simple and accessible to experimentation. The muscle cell is large enough to accommodate the two or more microelectrodes needed to make electrical measurements. Also the muscle cell normally receives signals from just one presynaptic axon, in contrast to the convergent connections on central nerve cells. Most importantly, chemical signaling at the nerve-muscle synapse involves a relatively simple mechanism: Release of neurotransmitter from the presynaptic nerve directly opens a single type of ion channel in the postsynaptic membrane.

The Neuromuscular Junction Is a Well-Studied Example of Directly Gated Synaptic Transmission

The motor neuron innervates the muscle at a specialized region of the muscle membrane called the *end-plate*, where the motor axon loses its myelin sheath and splits into several fine branches. The ends of the fine branches form multiple expansions or varicosities, called *synaptic boutons*, from which the motor neuron releases its transmitter. Each bouton is positioned over a specialized region of the muscle membrane containing deep depressions, or *junctional folds*, which contain the transmitter receptors (Figure 9–1). The transmitter released by the motor axon terminal is acetylcholine (ACh) and the receptor on the muscle membrane is the nicotinic type of ACh receptor.[1]

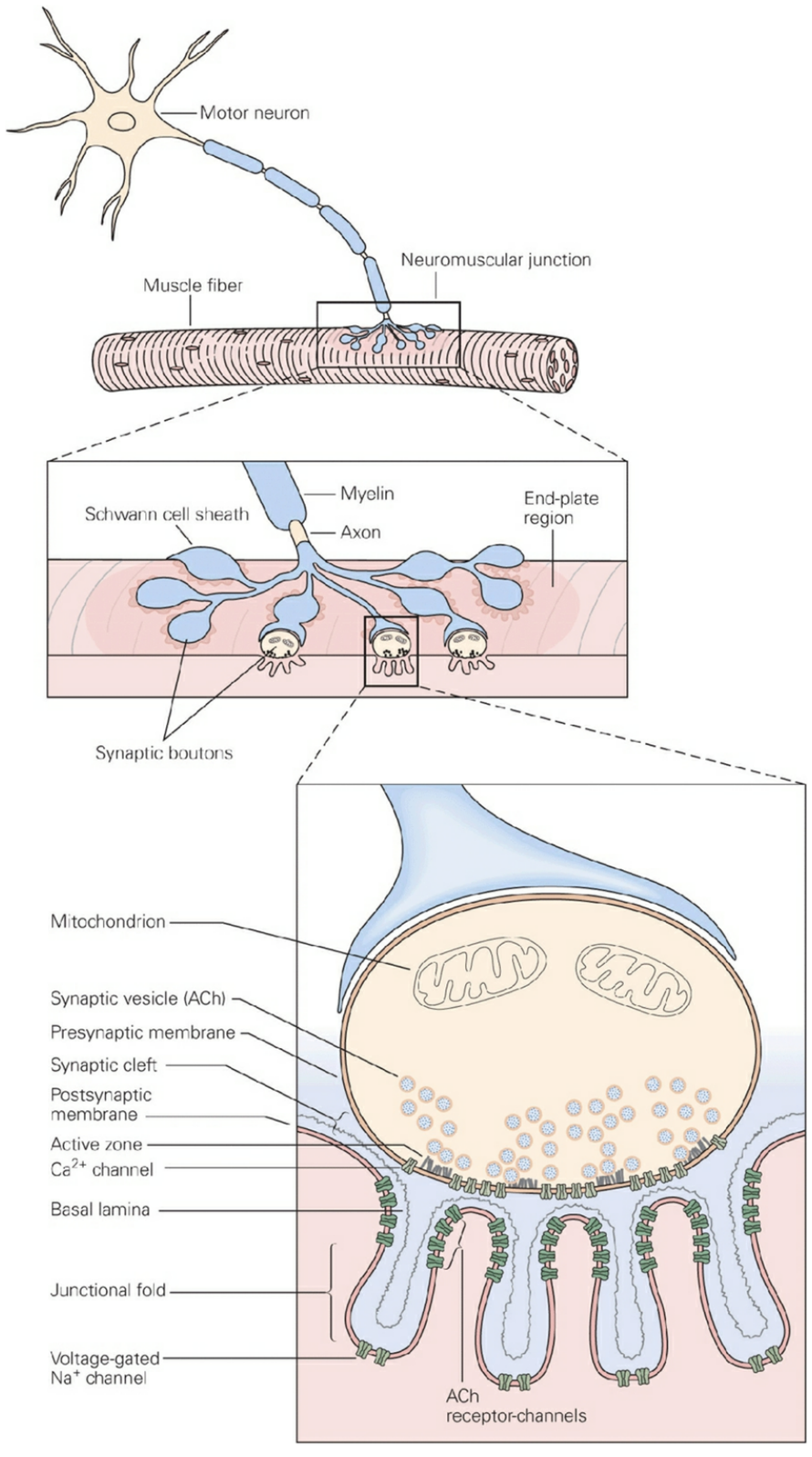

Figure 9-1 The neuromuscular junction is an ideal site for studying chemical synaptic signaling. At the muscle the motor axon ramifies into several fine branches approximately 2 μm thick. Each branch forms multiple swellings called *synaptic boutons*, which are covered by a thin layer of Schwann cells. The boutons lie over a specialized region of the muscle fiber membrane, the *end-plate*, and are separated from the muscle membrane by a 100-nm synaptic cleft. Each bouton contains mitochondria and synaptic vesicles clustered around *active zones*, where the neurotransmitter acetylcholine (ACh) is released. Immediately under each bouton in the end-plate are several junctional folds, the crests of which contain a high density of ACh receptors.

The muscle fiber and nerve terminal are covered by a layer of connective tissue, the basal lamina, consisting of collagen and glycoproteins. Unlike the cell membrane, the basal lamina is freely permeable to ions and small organic compounds, including the transmitter. Both the presynaptic terminal and the muscle fiber secrete proteins into the basal lamina, including the enzyme acetylcholinesterase, which inactivates the ACh released from the presynaptic terminal by breaking it down into acetate and choline. The basal lamina also organizes the synapse by aligning the presynaptic boutons with the postsynaptic junctional folds. (Adapted, with permission, from McMahan and Kuffler 1971.)

The presynaptic and postsynaptic membranes are separated by a synaptic cleft approximately 100 nm wide. Within the cleft is a basal lamina (or basement membrane) composed of collagen and other extracellular matrix proteins. The enzyme acetylcholinesterase, which rapidly hydrolyzes ACh, is anchored to the collagen fibrils of the basal laminae. In the muscle cell, in the region below the crest of the junctional fold and extending into the fold, the membrane is rich in voltage-gated Na^+ channels (Figure 9–1).

Each synaptic bouton contains all the machinery required to release neurotransmitter. This includes the synaptic vesicles, which contain the transmitter ACh, and the active zones, regions of the membrane specialized for release of transmitter, where the synaptic vesicles are clustered (Figure 9–1). In addition, each active zone contains voltage-gated Ca^{2+} channels that permit Ca^{2+} to enter the terminal with each action potential (see Figure 9-1). This influx of Ca^{2+} triggers the fusion of the synaptic

vesicles with the plasma membrane at the active zones, releasing the contents of the synaptic vesicle into the synaptic cleft by the process of exocytosis (see Chapter 12). Every active zone in the presynaptic membrane is positioned opposite a junctional fold in the postsynaptic cell. At the crest of each fold the receptors for ACh are clustered in a lattice, with a density of approximately 10,000 receptors per μm^2 (Figure 9–2). The nicotinic ACh receptor is a ligand-gated channel: It is an integral membrane protein that both binds ACh and forms an ion channel (Figure 9–3).

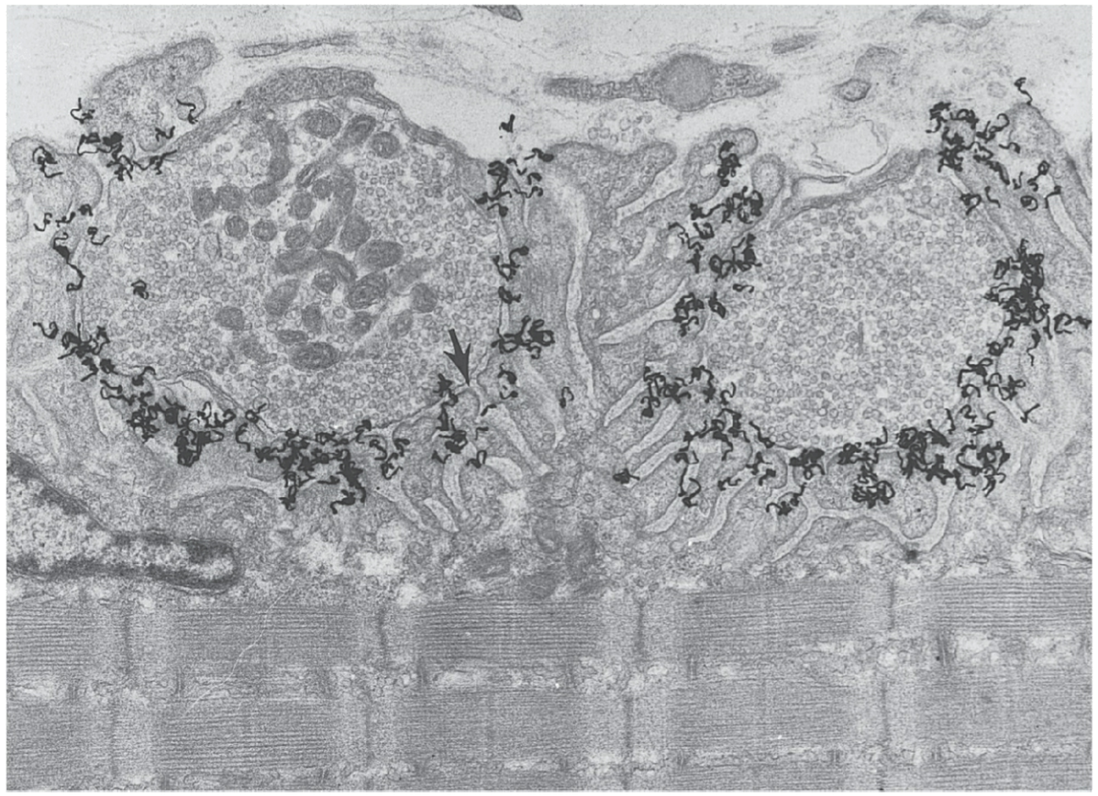

Figure 9-2 Acetylcholine receptors in the vertebrate neuromuscular junction are concentrated at the top one-third of the junctional folds. This receptor-rich region is characterized by an increased density of the postjunctional membrane (arrow). The autoradiograph shown here was made by first incubating the membrane with radiolabeled α-bungarotoxin, which binds to the ACh receptor (black grains). Radioactive decay results in the emittance of a particle that causes overlaid silver grains to become fixed along its trajectory (black grains). Magnification ×18,000. (Reproduced, with permission, from Salpeter 1987.)

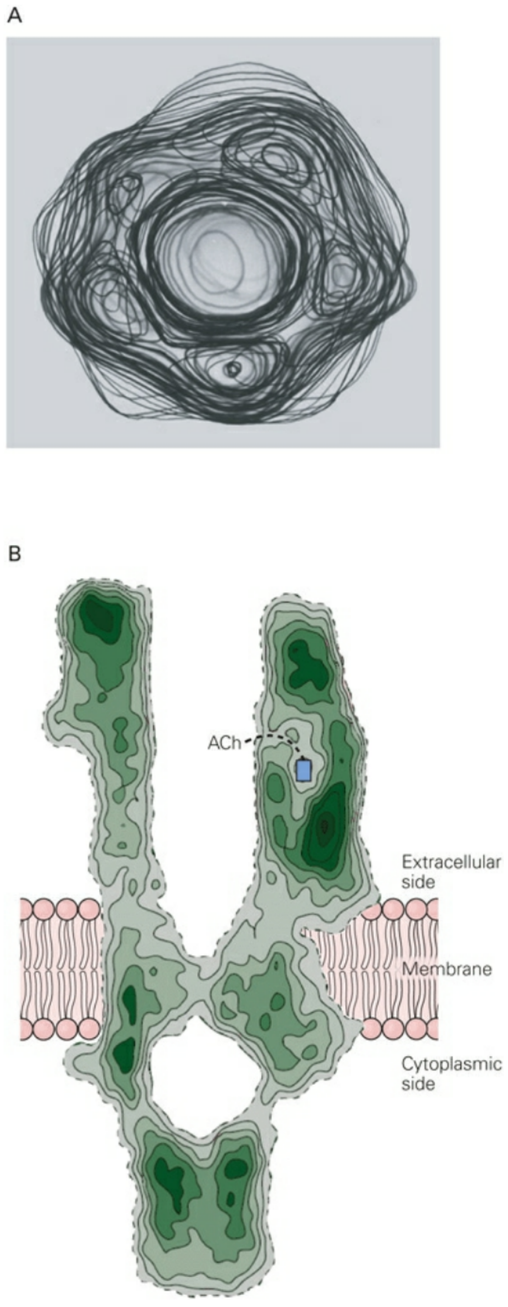

Figure 9-3 Low-resolution structure of the acetylcholine (ACh) receptor-channel. These reconstructed electron microscope images were obtained by computer processing of negatively stained images of ACh receptors in the fish *Torpedo californica*. The resolution is fine enough

to see overall structures but too coarse to resolve individual atoms.

A. View looking down on the receptor from the extracellular space. The overall diameter of the receptor and its channel is approximately 8.5 nm. (Reproduced, with permission, from Brisson and Unwin 1985.)

B. Side view of the receptor in the lipid bilayer. The pore is wide at the external and internal surfaces of the membrane but narrows considerably within the lipid bilayer. The channel extends some distance into the extracellular space. A molecule of ACh enters a crevice in the wall of the receptor. (Adapted, with permission, from Karlin 2002; Miyazawa et al. 1999.)

The Motor Neuron Excites the Muscle by Opening Ligand-Gated Ion Channels at the End-Plate

The release of transmitter from the motor nerve terminal opens ACh receptor-channels in the muscle membrane at the end-plate, and this action rapidly depolarizes the membrane. The resulting excitatory postsynaptic potential (EPSP), also called the *end-plate potential* at the nerve-muscle synapse, is very large; stimulation of a single motor cell produces a synaptic potential of approximately 70 mV.

This change in membrane potential usually is large enough to rapidly activate the voltage-gated Na^+ channels in the junctional folds, converting the end-plate potential into an action potential, which then propagates along the muscle fiber. In contrast, in the central nervous system most presynaptic neurons produce postsynaptic potentials less than 1 mV in amplitude. As a result, input from many presynaptic neurons is needed to generate an action potential in most neurons.

The End-Plate Potential Is Produced by Ionic Current Through Acetylcholine Receptor-Channels

The end-plate potential was first studied in detail in the 1950s by Paul Fatt and Bernard Katz using intracellular voltage recordings. Fatt and Katz were able to isolate the end-plate potential by applying the drug curare[2] to reduce the amplitude of the postsynaptic potential below the threshold for the action potential (Figure 9–4). They found that the EPSP in muscle cells was largest at the end-plate and decreased progressively with distance (Figure 9–5).

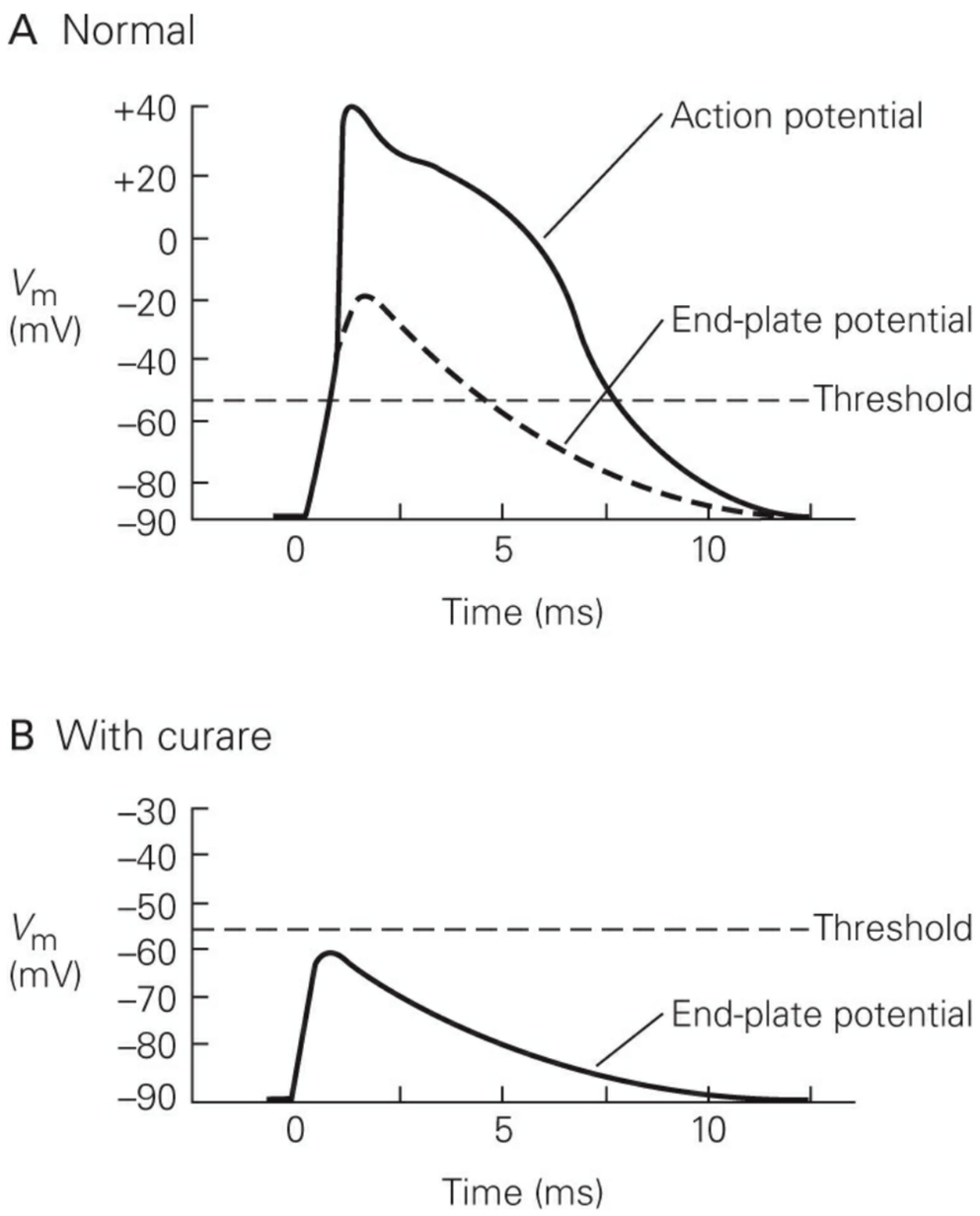

Figure 9-4 The end-plate potential can be isolated pharmacologically for study.

A. Under normal circumstances stimulation of the motor axon pro-

duces an action potential in a skeletal muscle cell. The **dashed line** shows the inferred time course of the end-plate potential that triggers the action potential.

B. Curare blocks the binding of acetylcholine (ACh) to its receptor and so prevents the end-plate potential from reaching the threshold for an action potential (dashed line). In this way the currents and channels that contribute to the end-plate potential, which are different from those producing an action potential, can be studied. The end-plate potential shown here was recorded in the presence of a low concentration of curare, which blocks only a fraction of the ACh receptors. The values for the resting potential (-90 mV), end-plate potential, and action potential in these intracellular recordings are typical of a vertebrate skeletal muscle.

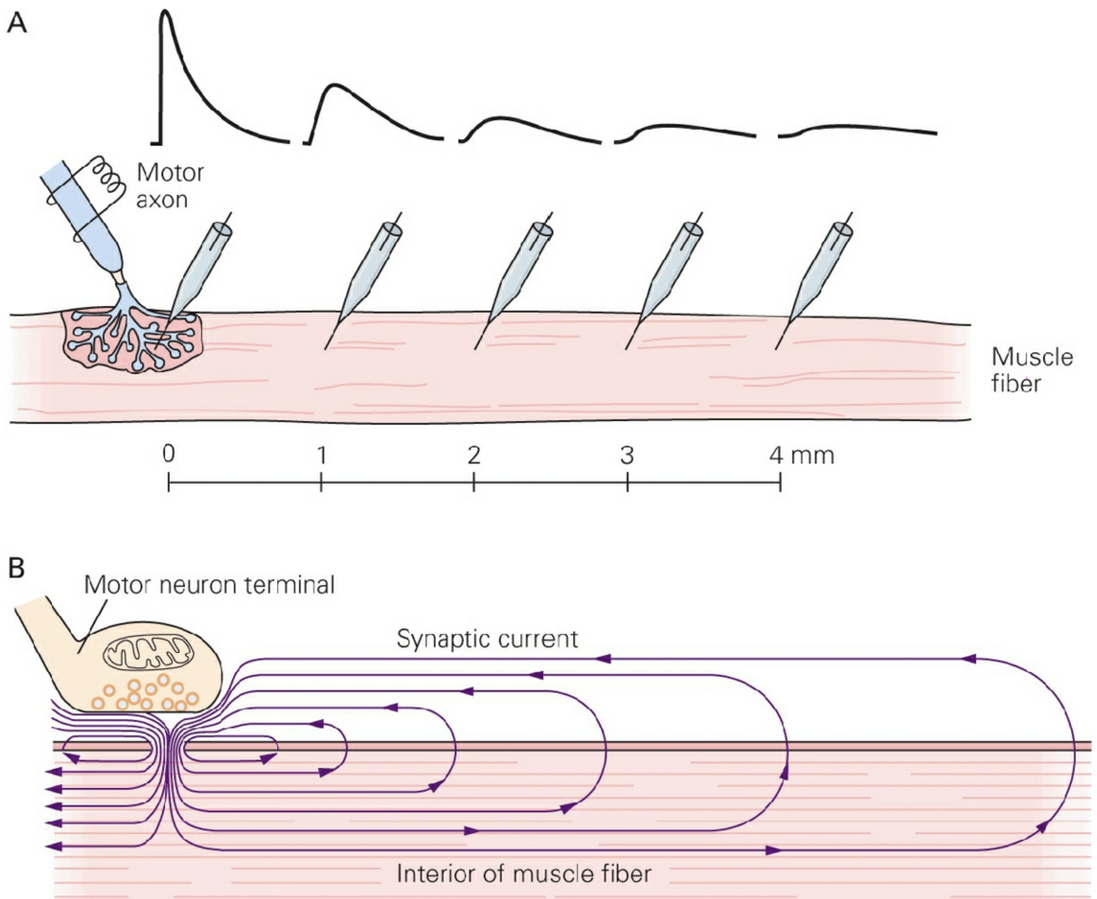

Figure 9-5 The end-plate potential decreases with distance as it passively propagates away from the end-plate. (Adapted, with permission, from Miles 1969.)

A. The amplitude of the postsynaptic potential decreases and the time course of the potential slows with distance from the site of initiation in the end-plate.

B. The decay results from leakiness of the muscle fiber membrane. Because charge must flow in a complete circuit, the inward synaptic current at the end-plate gives rise to a return outward current through resting channels and across the membrane (the capacitor). This return outward flow of positive charge depolarizes the membrane. Because current leaks out all along the membrane, the outward current decreases with distance from the end-plate.

From this, Fatt and Katz concluded that the end-plate potential is generated by an inward ionic current that is confined to the end-plate and then spreads passively away. (Remember, an inward current corresponds to an influx of positive charge, which depolarizes the inside of the membrane.) Inward current is confined to the end-plate because the ACh receptor-channels are concentrated there, opposite the presynaptic terminal from which transmitter is released.

The end-plate potential rises rapidly but decays more slowly. The rapid rise is caused by the sudden release into the synaptic cleft of ACh, which diffuses rapidly to the receptors at the end-plate. (Not all the ACh reaches receptors, however, because ACh is quickly removed from the synaptic cleft by hydrolysis by acetylcholinesterase and diffusion.)

The current that generates the end-plate potential was first studied in voltage-clamp experiments (see Box 7-1). These studies revealed that the end-plate current rises and decays more rapidly than the resultant end-plate potential (Figure 9–6). The time course of the end-plate current is directly determined by the rapid opening and closing of the ACh receptor-channels. Because it takes time for an ionic current to charge or discharge the muscle membrane capacitance, and thus alter the membrane voltage, the EPSP lags behind the synaptic current (see Figure 6-15 and the Postscript at the end of this chapter).

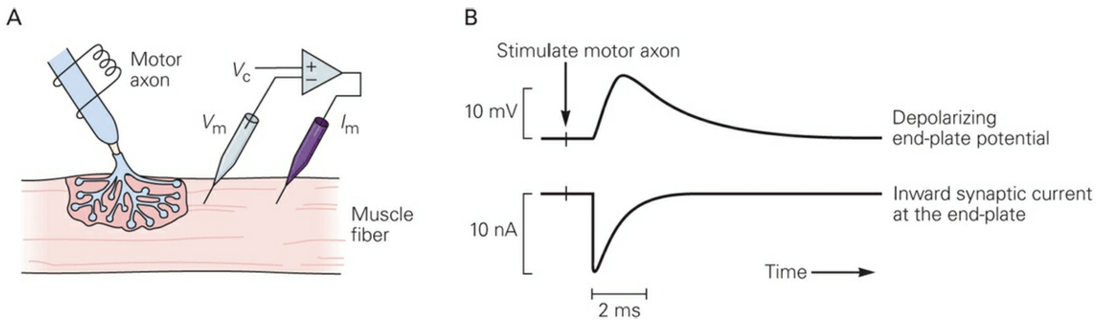

Figure 9-6 The end-plate current increases and decays more rapidly than the end-plate potential.

A. The membrane at the end-plate is voltage-clamped by inserting two microelectrodes into the muscle at the end-plate. One electrode measures membrane potential (V_m) and the second passes current (I_m). Both electrodes are connected to a negative feedback amplifier, which ensures that sufficient current (I_m) is delivered so that V_m will remain clamped at the command potential V_c. The synaptic current evoked by stimulating the motor nerve can then be measured at constant V_m, for example -90 mV (see Box 7-1).

B. The end-plate potential (measured when V_m is not clamped) changes relatively slowly and lags behind the more rapid inward synaptic current (measured under voltage-clamp conditions). This is because synaptic current must first alter the charge on the membrane capacitance of the muscle before the muscle membrane is depolarized.

The Ion Channel at the End-Plate Is Permeable to Both Sodium and Potassium

Why does the opening of the ACh receptor-channels lead to an inward current that produces the depolarizing end-plate potential? And which ions move through the ACh-gated channels to produce this inward current? One important means of identifying the ion (or ions) responsible for the synaptic current is to measure the value of the chemical driving force (the chemical battery) propelling ions through the channel. Remember, the current through a set of membrane channels is given by the product of the membrane conductance and the electrochemical driving force on the ions conducted through the channels (see Chapter 6). The end-plate current that underlies the EPSP is determined by:

$$I_{EPSP} = g_{EPSP} \times (V_m - E_{EPSP}), \qquad \textbf{(9–1)}$$

where I_{EPSP} is the end-plate current, g_{EPSP} is the conductance of the ACh receptor-channels, V_m is the membrane potential, and E_{EPSP} is the chemical driving force or battery generated by the transmembrane concentration gradients of the ions conducted through the channels.

The fact that current through the end-plate is inward at the normal resting potential of a muscle cell (-90 mV) indicates that there is an inward (negative) electrochemical driving force on the ions that carry current through the ACh receptor-channels at this potential. Thus, E_{EPSP} must be positive to -90 mV.

The value of E_{EPSP} in Equation 9–1 can be determined by altering V_m in a voltage-clamp experiment and determining its effect on I_{EPSP}. Depolarizing the membrane reduces the net inward electrochemical driving force, thus decreasing the magnitude of the inward end-plate current. If V_m is set equal to E_{EPSP}, there will be no net current through the end-plate channels because the electrical driving force (V_m) will exactly balance the chemical driving force (E_{EPSP}). The potential at which the net ionic current is zero is the *reversal potential* for current through the synaptic channels; by determining the reversal potential we can experimentally measure the value of E_{EPSP}. If V_m is made more positive than E_{EPSP}, there will be a net outward driving force. In that case stimulation of the motor nerve leads to an outward ionic current (by opening the ACh receptor-channels) that hyperpolarizes the membrane.

If an influx of Na^+ were solely responsible for the end-plate potential, the reversal potential for the excitatory postsynaptic potential would be the same as the equilibrium potential for Na^+ $Na^+(E_{Na} = +55\ mV)$. Thus, if V_m is experimentally altered from -100 to +55 mV, the end-plate current should diminish progressively because the electrochemical driving force on Na^+ $(V_m - E_{Na})$ is reduced. At +55 mV the inward current should be abolished, and at potentials more positive than +55 mV the end-plate current should reverse in direction and become outward.

Instead, experiments at the end-plate showed that as V_m is reduced, the inward current rapidly becomes smaller and is abolished at 0 mV. At values more positive than 0 mV the end-plate current reverses direction

and becomes outward (Figure 9–7). This reversal potential is not equal to the equilibrium potential for Na^+ or any of the other major cations or anions. In fact, this chemical potential is produced not by a single ion species but by a combination of ions: The ligand-gated channels at the end-plate are almost equally permeable to both major cations, Na^+, and K^+. Thus, during the end-plate potential Na^+ flows into the cell and K^+ flows out. The reversal potential is at 0 mV because this is a weighted average of the equilibrium potentials for Na^+, and K^+ (Box 9-1). At the reversal potential the influx of Na^+ is balanced by an equal efflux of K^+ (Figure 9–7).

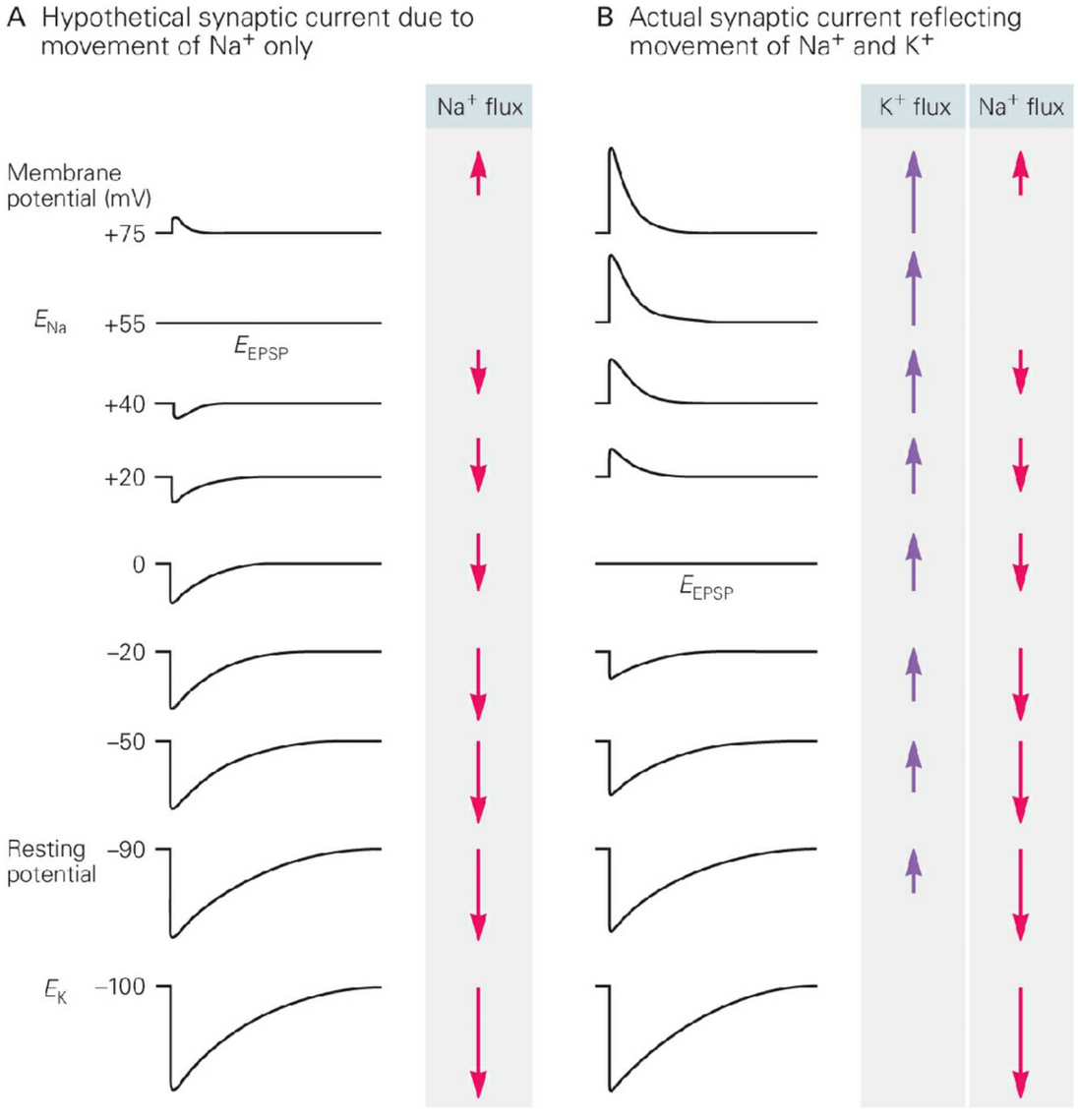

Figure 9-7 The end-plate potential is produced by the simultaneous flow of Na^+, and K^+ through the same receptor-channels. The ionic currents responsible for the end-plate potential can be determined by measuring the reversal potential of the end-plate current using a voltage clamp.

A. In the hypothetical case in which Na^+ flux alone is responsible for the end-plate current, the reversal potential would occur at +55 mV, the equilibrium potential for Na^+ (E_{Na}). The arrow at the right of each current record reflects the magnitude of the net Na^+ flux at that membrane potential. (Down arrows = inward; up arrows = outward).

B. In the actual case in which the ACh receptor-channel is permeable to both Na^+, and K^+, experimental results show that the end-plate current reverses at 0 mV because the ion channel allows Na^+, and K^+ to move into and out of the cell simultaneously (see Box 9-1). The net current is the sum of the Na^+, and K^+ fluxes through the end-plate channels. At the reversal potential (E_{EPSP}) the inward Na^+ flux is balanced by an outward K^+ flux so that no net charge flows.

Why are the ACh receptor-channels at the end-plate not selective for a single ion species like the voltage-gated Na^+ or K^+ channels? This is because the diameter of the pore of the ACh receptor-channel is substantially larger than that of the voltage-gated channels. Electrophysiological measurements suggest that it may be up to 0.8 nm in diameter, an estimate based on the size of the largest organic cation that can permeate the channel. For example, the permeant cation tetramethylammonium (TMA) is approximately 0.6 nm in diameter. In contrast, the voltage-gated Na^+ channel is only permeant to organic cations that are smaller than 0.5 × 0.3 nm in cross section, and voltage-gated K^+ channels will only conduct ions less than 0.3 nm in diameter.

The relatively large diameter of the ACh receptor pore is thought to provide a water-filled environment that allows cations to diffuse through the channel relatively unimpeded, much as they would in free solution. This explains why the pore does not discriminate between Na^+, and K^+. It also explains why even divalent cations, such as Ca^{2+}, can permeate the channel. Anions are excluded, however, by the presence of fixed negative charges in the channel, as described later in this chapter.

The Current Through Single Acetylcholine Receptor-Channels Can Be Measured Using the Patch Clamp

The synaptic current at the end-plate is generated by a couple of hundred thousand channels. Recordings of the current through single ACh receptor-channels, using the patch-clamp technique (see Box 5-1), have provided us with insight into the molecular events underlying the end-plate potential.

Individual Receptor-Channels Conduct All-or-None Unitary Currents

The first successful recordings of single ACh receptor-channel currents from skeletal muscle cells, by Erwin Neher and Bert Sakmann in 1976, showed that the opening of an individual channel generates a very small rectangular step of ionic current (Figure 9–8). At a given resting potential a channel will always generate the same-size current pulse. At -90 mV the current steps are approximately -2.7 pA in amplitude. Although this is a very small current, it corresponds to a flow of approximately 17 million ions per second!

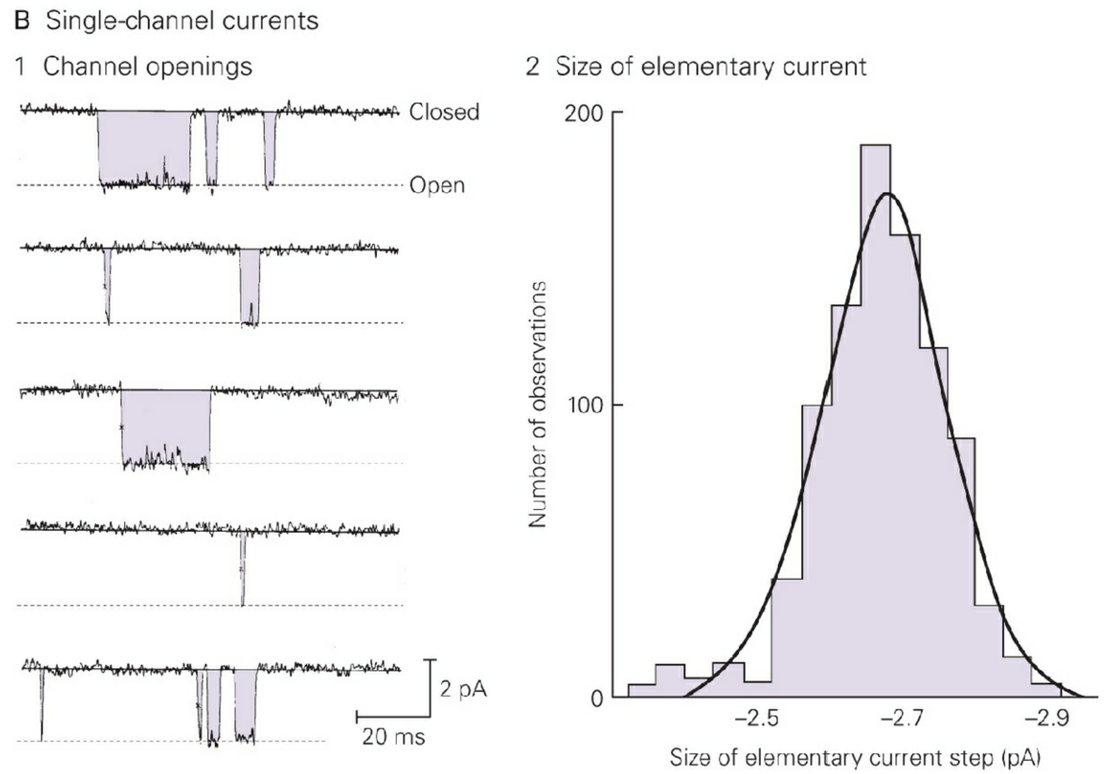

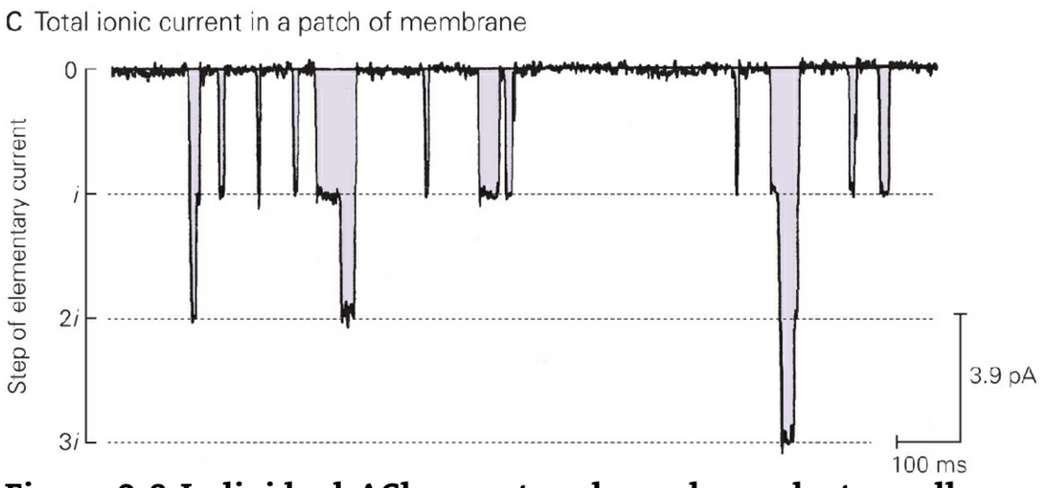

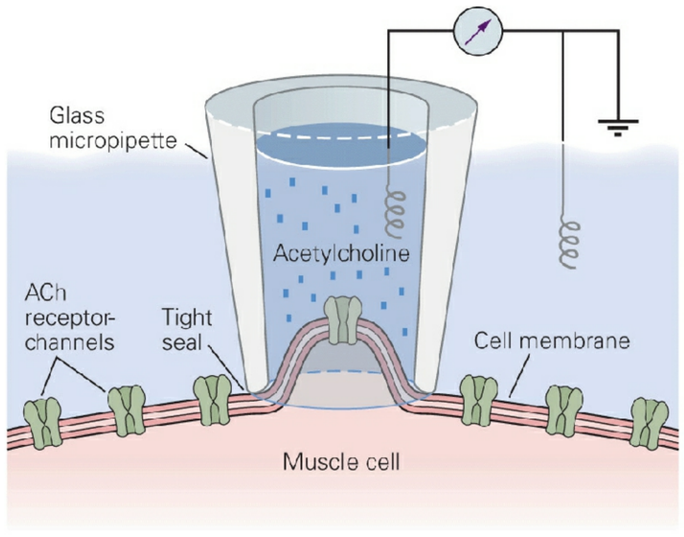

Figure 9-8 Individual ACh receptor-channels conduct an all-or-none elementary current.

A. The patch-clamp technique is used to record currents from single ACh receptor-channels. The patch electrode is filled with salt solution that contains a low concentration of ACh and is then brought into close

contact with the surface of the muscle membrane (see Box 5-1). The patch may contain one or many receptor-channels.

B. Single-channel currents from a patch of frog muscle membrane with a resting potential of -90 mV were recorded in the presence of 100 nM ACh. (**1**) The opening of a channel results in an influx of positive charge (recorded as a downward current step). The patch contained a large number of ACh receptor-channels so that successive openings in the record probably arise from different channels. (**2**) A histogram plotting the amplitudes of these rectangular pulses (in pA) versus the number of observed pulses with the given amplitude. The histogram has a single peak, indicating that the patch of membrane contains only a single type of active channel with an elementary current that varies randomly around a mean of -2.7 pA (1 pA = 10^{-12} A). This mean, the *elementary current*, represents an elementary conductance of 30 pS. (Reproduced, with permission, from B. Sakmann.)

C. When the membrane potential is increased to -130 mV, the individual channel currents increase to -3.9 pA because of the increase in electrical driving force. The elementary conductance remains equal to 30 pS. When several channels open simultaneously, the individual current pulses add linearly. The record shows one, two, or three channels open at different times in response to application of ACh. (Reproduced, with permission, from B. Sakmann.)

The current steps change in size with changes in membrane potential because the current depends on the electrochemical driving force $(V_m - E_{EPSP})$. For single ion channels the equivalent of Equation 9–1 is

$$i_{EPSP} = \gamma_{EPSP} \times (V_m - E_{EPSP}),$$

where i_{EPSP} is the amplitude of current through one channel and γ_{EPSP} is the conductance of a single channel. The relationship between i_{EPSP} and membrane voltage is linear, indicating that the single-channel conductance is constant and does not depend on membrane voltage; that is, the channel behaves as a simple resistor. From the slope of this relation the channel is found to have a conductance of 30 pS. The reversal potential of 0 mV, obtained from the intercept of the membrane voltage axis, is identical to that for the end-plate current (Figure 9–9B).

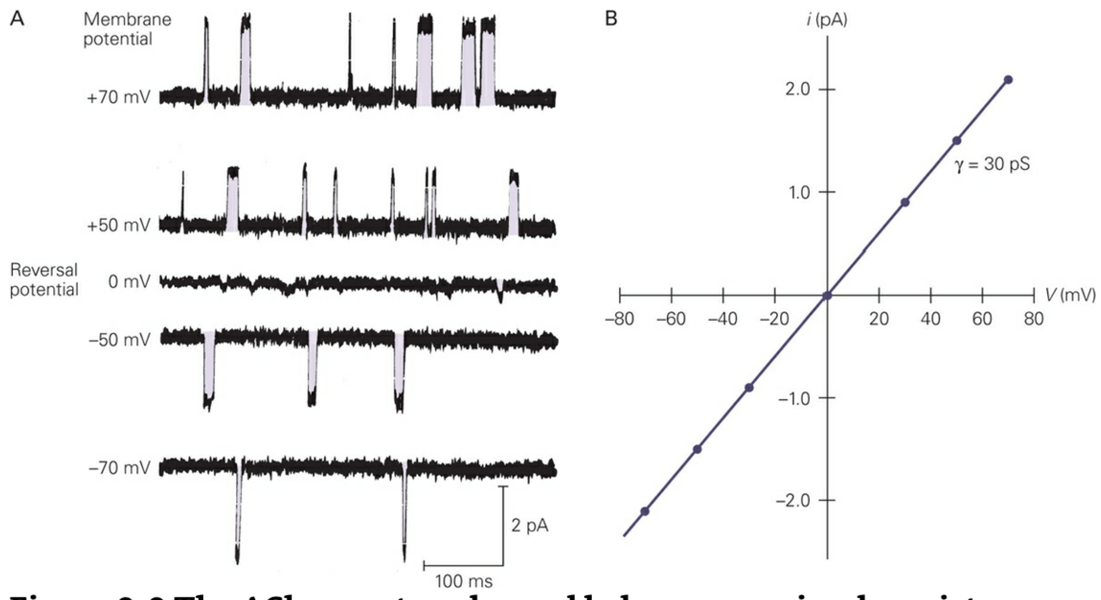

Figure 9-9 The ACh receptor-channel behaves as a simple resistor.

A. The voltage across a patch of membrane was systematically varied during exposure to 2 μM ACh. The current recorded at the patch is inward at voltages negative to 0 mV and outward at voltages positive to 0 mV, thus defining 0 mV as the reversal potential.

B. The linear relation between current through a single ACh receptor-channel and membrane voltage shows that the channel behaves as a simple resistor with a single-channel conductance (γ) of about 30 pS.

Box 9–1 Reversal Potential of the End-Plate Potential

The reversal potential of a membrane current carried by more than one ion species, such as the end-plate current through the ACh receptor-channel, is determined by two factors: (1) the relative conductance for the permeant ions (g_{Na} and g_K in the case of the end-plate current) and (2) the equilibrium potentials of the ions (E_{Na} and E_K).

At the reversal potential for the ACh-gated current, inward current carried by Na^+ is balanced by outward current carried by K^+:

$$I_{Na} + I_K = 0. \qquad (9–2)$$

The individual Na^+, and K^+ currents can be obtained from

$$I_{Na} = g_{Na} \times (V_m - E_{Na}) \qquad (9–3a)$$

and

$$I_K = g_K \times (V_m - E_K). \qquad \textbf{(9–3b)}$$

Remember that these currents do not result from Na^+, and K^+ flowing through separate channels (as occurs during the action potential) but through the same ACh receptor-channel. We can substitute Equations 9–3a and 9–3b for I_{Na} and I_K in Equation 9–2, replacing V_m with E_{EPSP} (because at the reversal potential $V_m = E_{EPSP}$):

$$g_{Na} \times (E_{EPSP} - E_{Na}) + g_K \times (E_{EPSP} - E_K) = 0. \qquad \textbf{(9–4)}$$

Solving this equation for E_{EPSP} yields

$$E_{EPSP} = \frac{(g_{Na} \times E_{Na}) + (g_K \times E_K)}{g_{Na} + g_K}. \qquad \textbf{(9–5)}$$

If we divide the top and bottom of the right side of this equation by g_K, we obtain

$$E_{EPSP} = \frac{E_{Na}\,(g_{Na}/g_K) + E_K}{(g_{Na}/g_K) + 1}. \qquad \textbf{(9–6)}$$

If $g_{Na} = g_K$, then $E_{EPSP} = (E_{Na} + E_K)/2$.

These equations can also be used to solve for the ratio g_{Na}/g_K if one knows E_{EPSP}, E_K, and E_{Na}. Thus, rearranging Equation 9–6 yields

$$\frac{g_{Na}}{g_K} = \frac{E_{EPSP} - E_K}{E_{Na} - E_{EPSP}}. \qquad \textbf{(9–7)}$$

At the neuromuscular junction, $E_{EPSP} = 0$ mV, $E_K = -100$ mV, and $E_{Na} = +55$ mV. Thus, from Equation 9–7, g_{Na}/g_K has a value of approximately 1.8, indicating that the conductance of the ACh receptor-channel for Na^+ is slightly higher than for K^+. A comparable approach can be used to analyze the reversal potential and the movement of ions during excitatory and inhibitory synaptic potentials in central neurons (see Chapter 10).

Although the amplitude of the current through a single ACh channel is constant for every opening, the duration of each opening and the time between openings vary considerably. These variations occur because channel openings and closings are stochastic; they obey the same statistical law that describes radioactive decay. Because of the random thermal motions and fluctuations that a channel experiences, it is impossible to predict exactly how long it will take any one channel to bind ACh or how long that channel will stay open before the ACh dissociates and the channel closes. However, the average length of time a particular type of channel stays open is a well-defined property of that channel, just as the half-life of radioactive decay is an invariant property of a particular isotope. The mean open time for ACh receptor-channels is approximately 1 ms. Thus each channel opening permits the movement of approximately 17,000 ions.

Each ACh receptor-channel has two binding sites for ACh; both sites must be occupied by transmitter for the channel to open efficiently. Once a channel closes, the ACh molecules dissociate and the channel remains closed until it binds ACh again.

Four Factors Determine the End-Plate Current

Stimulation of a motor nerve releases a large quantity of ACh into the synaptic cleft. The ACh rapidly diffuses across the cleft and binds to the ACh receptors, causing more than 200,000 receptor-channels to open almost simultaneously. (This number is obtained by comparing the total end-plate current, approximately -500 nA, with the current through a single channel, approximately -2.7 pA.) How do small step-like changes in current through 200,000 individual ACh receptor-channels produce the smooth waveform of the end-plate current?

The rapid opening of so many channels causes a large increase in the total conductance of the end-plate membrane, g_{EPSP}, and produces the rapid increase in end-plate current. The ACh in the cleft decreases rapidly to zero (in less than 1 ms) because of enzymatic hydrolysis and diffusion, after which the channels begin to close in the random manner described above. Each closure produces a small step-like decrease in end-plate current because of the all-or-none nature of single-channel currents. However, because each unitary current step is tiny relative to the large current carried by many thousands of channels, the random closing of a large number of small unitary currents causes the total end-plate current to appear to decay smoothly (Figure 9–10).

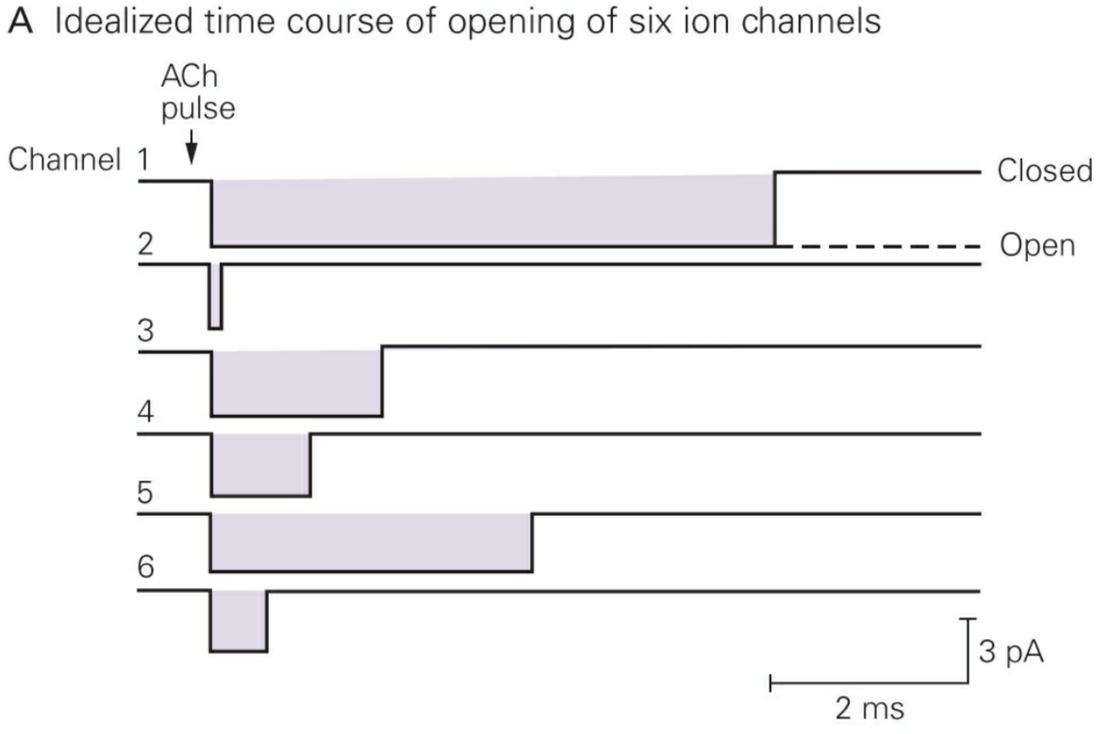

Figure 9-10 The time course of the total current at the end-plate results from the summed contributions of many individual ACh receptor-channels. (Reproduced, with permission, from Colquhoun 1981.)

A. Individual ACh receptor-channels open in response to a brief pulse of ACh. In this idealized example the membrane contains a total of six ACh receptor-channels. All channels open rapidly and nearly simultaneously. The channels remain open for varying times and close independently.

B. The stepped trace shows the sum of the six single-channel current records in part A. It represents the current during the sequential closing of each channel (the number indicates which channel has closed) in a hypothetical end-plate containing only six channels. In the final period of current only channel 1 is open. In a current record from a whole muscle fiber, with thousands of channels, the individual channel closings are not visible because the current scale needed to display the total end-plate current (hundreds of nanoamperes) is so large that the contributions of individual channels cannot be resolved. As a result, the total end-plate current appears to decay smoothly.

The summed conductance of all open channels in a large population of ACh receptor-channels is the total synaptic conductance, $g_{EPSP} = n \times \gamma$, where n is the average number of channels opened and γ is the conductance of a single channel. The number of open channels is the product of the total number of channels in the end-plate membrane (N) and the probability that any given channel is open, $n = N \times p_{open}$. The probability that a channel is open depends largely on the concentration of the transmitter at the receptor, not on the value of the membrane potential, because the channels are opened by the binding of ACh, not by voltage. The total end-plate current is therefore given by

$$I_{EPSP} = N \times p_{open} \times \gamma \times (V_m - E_{EPSP}),$$
$$= n \times \gamma \times (V_m - E_{EPSP}).$$

This equation shows that the total end-plate current depends on four factors: (1) the total number of end-plate channels (N); (2) the probability that a channel is open (p_{open}); (3) the conductance of each open channel (γ); and (4) the driving force on the ions $(V_m - E_{EPSP})$.

The relationships between total end-plate current, end-plate potential, and single-channel current are shown in Figure 9–11 for a wide range of membrane potentials.

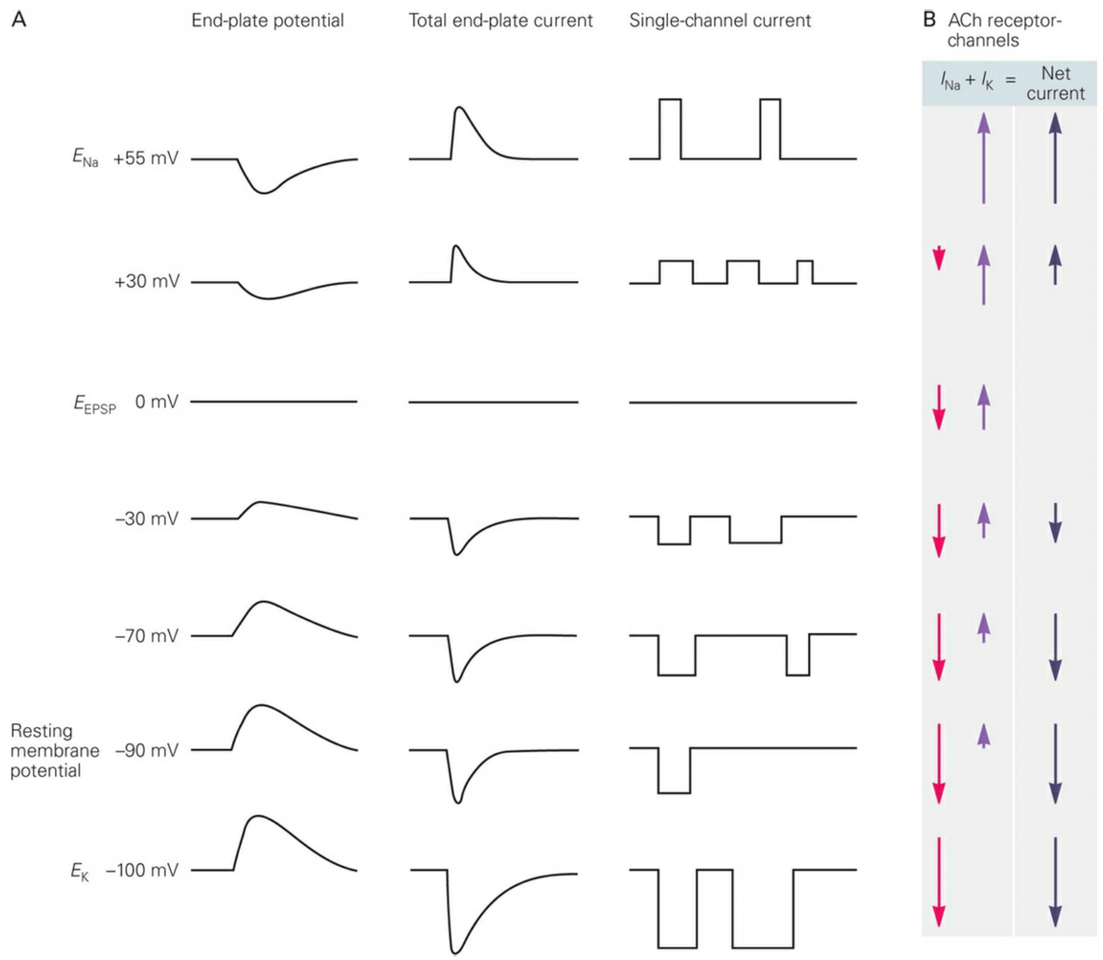

Figure 9-11 Membrane potential has a similar effect on the end-plate potential, total end-plate current, and ACh-gated single-channel current.

A. At the normal resting potential of the muscle membrane (-90 mV) the current through single ACh receptor-channels is large and inward because of the large inward driving force on Na^+, and small outward driving force on K^+. The resulting total end-plate current (made up of currents from more than 200,0000 channels) produces a large depolarizing end-plate potential. At more positive levels of membrane potential (increased depolarization), the inward driving force on Na^+ is less and the outward driving force on K^+ is greater. This results in a decrease in the size of the single-channel and total end-plate current, thus reducing the size of the end-plate potential. At the reversal potential (0 mV) the inward Na^+ flux is balanced by the outward K^+ flux, so there is no net current at the end-plate and no change in V_m. Further depolarization to +30 mV inverts the direction of the end-plate current, as there is now a much larger outward driving force on K^+, and a small inward driving force on Na^+. As a result, the outward flow of K^+ hyperpolarizes the membrane. Note that on either side of the reversal potential the end-plate current drives the membrane potential toward the reversal potential.

B. The direction of Na^+, and K^+ fluxes in individual channels changes with V_m. The algebraic sum of the Na^+, and K^+ currents, I_{Na} and I_K, gives the *net current* through the ACh receptor-channels. (Arrow length represents the relative magnitude of a current. Up = out, down = in.)

The Molecular Properties of the Acetylcholine Receptor-Channel Are Known

The ACh receptors that produce the end-plate potential differ in two important ways from the voltage-gated channels that generate the action potential in muscle. First, the action potential is generated by two distinct classes of voltage-gated channels that are activated sequentially, one selective for Na^+, and the other for K^+. In contrast, the ACh receptor-channel alone generates the end-plate potential by allowing both Na^+, and K^+ to pass with nearly equal permeability.

Second, the Na^+ flux through voltage-gated channels is regenerative: By increasing the depolarization of the cell, the Na^+ influx opens more voltage-gated Na^+ channels. This regenerative feature is responsible for the all-or-none property of the action potential. In contrast, the number of ACh receptor-channels opened during the synaptic potential is fixed by the amount of ACh available. The depolarization produced by Na^+ influx through these ligand-gated channels does not lead to the opening of more ACh-gated channels and cannot produce an action potential. To trigger an action potential, a synaptic potential must recruit neighboring voltage-gated channels (Figure 9–12).

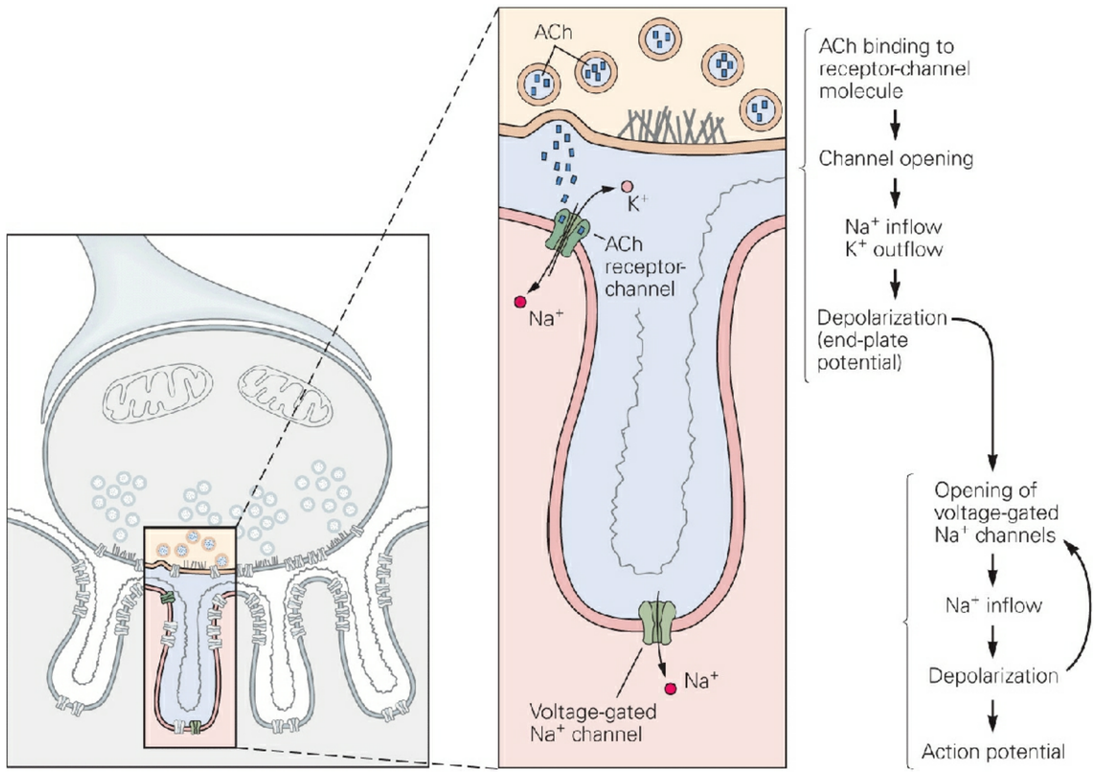

Figure 9-12 The depolarization resulting from the opening of ACh receptor-channels at the end-plate opens voltage-gated Na^+ channels. The depolarization of the muscle membrane during the end-plate potential opens neighboring voltage-gated Na^+ channels in the muscle membrane. The depolarization is normally large enough to open a sufficient number of Na^+ channels to exceed the threshold for an action potential. (Reproduced, with permission, from Alberts et al. 1989.)

As might be expected from these two differences in physiological properties, the ACh-gated and voltage-gated channels are formed by different macromolecules that exhibit different sensitivities to drugs and toxins. Tetrodotoxin, which blocks the voltage-gated Na^+ channel, does not block the influx of Na^+ through the nicotinic ACh receptor-channels. Similarly, α-bungarotoxin, a snake venom protein that binds tightly to the nicotinic receptors and blocks the action of ACh, does not interfere with voltage-gated Na^+ or K^+ channels (α-bungarotoxin has proved useful in the biochemical characterization of the ACh receptor).

The nicotinic ACh receptor at the nerve-muscle synapse is an ionotropic receptor: It is part of a single macromolecule that includes the pore in the membrane through which ions flow. Where in the molecule is the binding site located? How is the pore of the channel formed? What are its properties? Insights into these questions have been obtained from molecular studies of the ACh receptor proteins and their genes.

Biochemical studies by Arthur Karlin and Jean-Pierre Changeux indicate that the mature nicotinic ACh receptor is a membrane glycoprotein formed from five subunits: two α-subunits and one β-, one γ-, and one Δ-subunit. The amino terminus of each of the subunits is exposed on the extracellular surface of the membrane and contains the ACh-binding site. Karlin and his colleagues have identified two extracellular binding sites for ACh on each receptor-channel in the clefts between each α-subunit and its neighboring γ- or Δ-subunit. One molecule of ACh must bind at each of the two sites for the channel to open efficiently (Figure 9–13). The inhibitory snake venom α-bungarotoxin also binds to the ACh-binding sites on the α-subunit.

Insight into the structure of the channel has come from analysis of the primary amino acid sequences of the receptor's subunits as well as from biophysical studies. The work of Shosaku Numa and his colleagues demonstrated that the four subunit types are encoded by distinct but related genes. Sequence comparison of the subunits shows a high degree of similarity among them: One-half of the amino acid residues are identical or conservatively substituted. This similarity suggests that all subunits have a similar structure. Furthermore, all four of the genes for the subunits are homologous; that is, they are derived from a common ancestral gene.

The distribution of the polar and nonpolar amino acids of the subunits provides important clues as to how the subunits are threaded through the membrane bilayer. Each subunit contains four hydrophobic regions of approximately 20 amino acids called M1 to M4, each of which is thought to form an α-helix that spans the membrane. The amino acid sequences of the subunits suggest that the subunits are symmetrically arranged like the staves of a barrel, creating a central pore through the membrane (Figure 9–14).

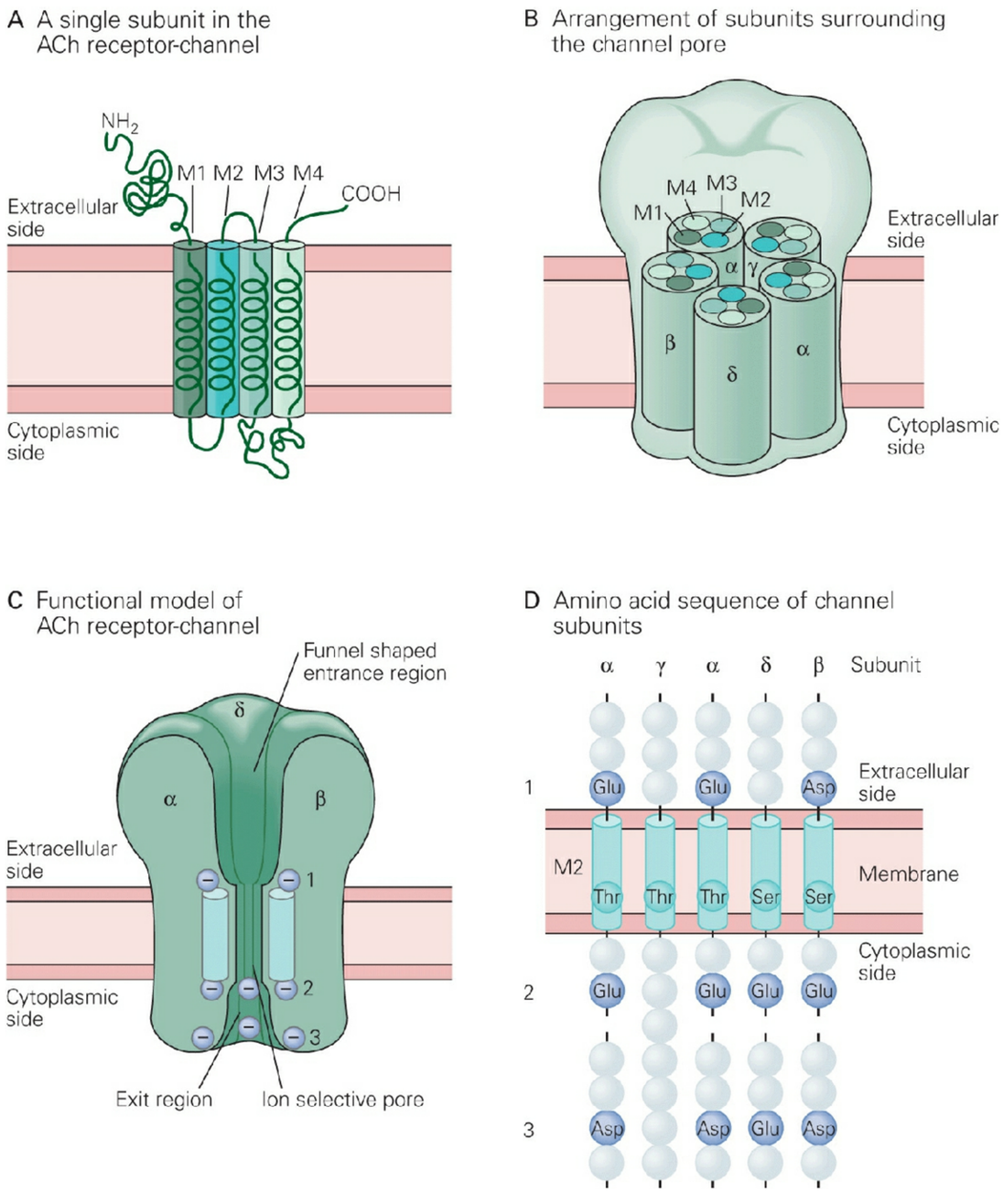

Figure 9-14 The ACh receptor subunits are homologous membrane-spanning proteins.

A. Each subunit contains a large extracellular N-terminus, four membrane-spanning α-helixes (**M1–M4**), and a short extracellular C-terminus. The N-terminus contains the ACh-binding site, and the membrane helixes form the pore.

B. The five subunits are arranged such that they form a central aqueous channel, with the M2 segment of each subunit forming the lining of the pore. Note that the γ-subunit lies between the two α-subunits. (Dimensions are not to scale.)

C. According to one model, negatively charged amino acids on each subunit form three rings of negative charge around the pore. As an ion traverses the channel it encounters these rings of charge. The rings at the external (**1**) and internal (**3**) surfaces of the cell membrane may serve as prefilters that help repel anions and form divalent cation blocking sites. The central ring near the cytoplasmic side of the membrane bilayer (**2**) may contribute more importantly to establishing the specific cation selectivity of the selectivity filter, which is the narrowest region of the pore.

D. The amino acid sequences of the M2 and flanking regions of each of the five subunits. The horizontal series of amino acids numbered **1, 2, and 3** constitute the three rings of negative charge (part C). The aligned serine and threonine residues within M2 help form the selectivity filter.

The walls of the channel pore are formed by the M2 membrane-spanning segment and by the loop connecting M2 to M3. Three rings of negative charges that flank the external and internal boundaries of the M2 segment play an important role in the channel's selectivity for cations. Certain local anesthetic drugs block the channel by interacting with one ring of polar serine residues and two rings of hydrophobic residues in the central region of the M2 helix, midway through the membrane (Figure 9-14D).

A three-dimensional model of the entire receptor-channel complex has been proposed by Arthur Karlin and Nigel Unwin based on neutron scattering and electron diffraction images respectively (see Figure 9-3). The complex is divided into three regions: a large extracellular portion that contains the ACh binding site, a narrow transmembrane pore selective for cations, and a large exit region at the internal membrane surface (Figure 9-14C). The extracellular region is surprisingly large, approximately 6 nm in length. In addition, the extracellular end of the pore has a wide mouth approximately 2.5 nm in diameter. Within the bilayer of the membrane the pore gradually narrows.

More detailed insight into the structure of the extracellular domain of the ACh receptor has come from X-ray crystallographic studies of a molluscan ACh-binding protein, which is homologous to the amino terminus of the nicotinic ACh receptor subunit at the end-plate. Remarkably, unlike typical ACh receptors, the molluscan ACh-binding protein is a soluble protein secreted by glial cells into the extracellular space. At cholinergic synapses in snails it acts to reduce the size of the excitatory postsynaptic potential, perhaps by buffering the free concentration of ACh in the synaptic cleft.

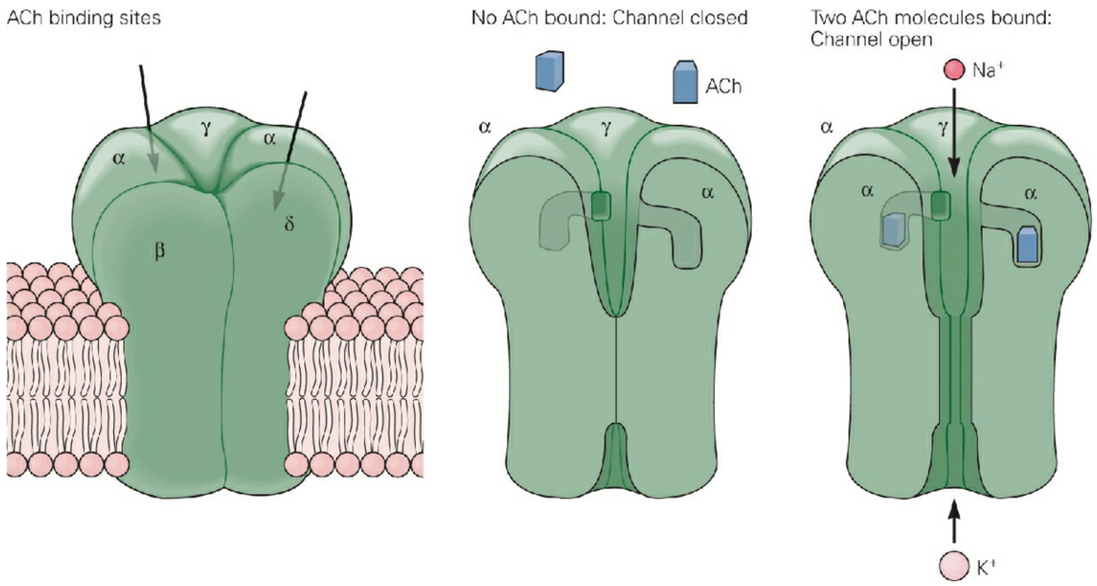

Figure 9-13 The nicotinic ACh receptor-channel is a pentameric macromolecule. The receptor-channel is a single macromolecule consisting of five subunits, which form a pore through the cell membrane (see Figure 9-14). The channel is composed of two identical αsubunits, and one each of the β-, γ-, and Δ-subunits. When two molecules of ACh bind to the extracellular binding sites—formed at the interfaces of the two α-subunits and their neighboring γ- and Δ-subunits—the receptor-channel molecule changes conformation. This change opens the pore through which both K^+, and Na^+ flow down their electrochemical gradients.

In a crystal structure of the molluscan ACh-binding protein in the presence of nicotine, five identical subunits are assembled into a symmetric pentameric ring (Figure 9–15A). The walls of the protein are seen to surround a large vestibule, which presumably funnels ions toward the narrow transmembrane domain of the receptor. Each subunit binds one molecule of nicotine at the ACh binding site, which is located at the interface between neighboring subunits; thus, the pentamer binds a total of five molecules of ligand. Although nicotinic ACh receptors at the end-plate have only two binding sites for ligand, some neuronal nicotinic ACh receptors are composed of five identical subunits and are thought to bind five molecules of ACh. Although the overall similarity of the amino acid sequences of the molluscan protein and nicotinic ACh receptors is fairly low (25%), the residues that form the ACh binding site are highly conserved, suggesting that the structure of the site is similar to that of the molluscan protein.

Our picture of the transmembrane region of the nicotinic ACh receptor is still incomplete. However, recent electron diffraction data from Unwin suggest that the four transmembrane segments of each subunit are indeed α-helixes that traverse the 3 nm length of the lipid bilayer (Figure 9-15B). The pore-lining M2 segments are inclined toward the central axis of the channel, so that the pore narrows continuously from the outside of the membrane to the inside. In the closed state a ring of hydrophobic residues is thought to constrict the pore in the middle of the M2 helix to a diameter of less than 0.6 nm. This hydrophobic ring may act as the channel's gate, providing a steric and energetic barrier that prevents ion conduction.

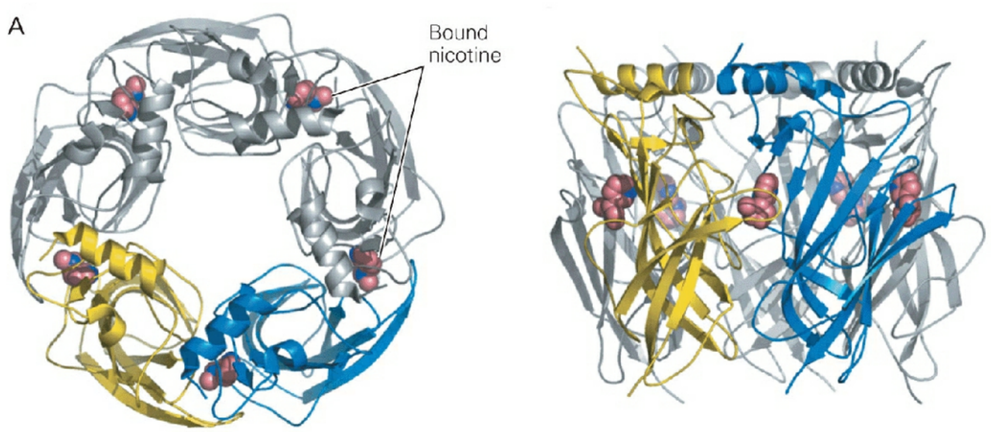

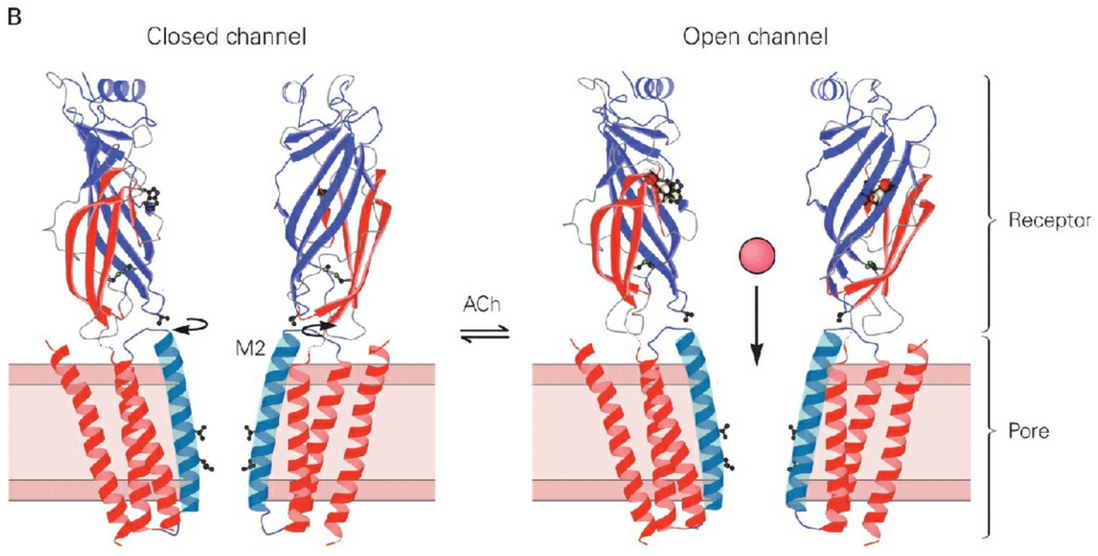

Figure 9-15 A high-resolution three-dimensional structural model of the nicotinic ACh receptor-channel.

A. A structural model of the ACh-binding protein, secreted by glial cells in mollusks, in the presence of nicotine. Five identical subunits assemble into a pentameric macromolecule that contains a large central cavity. The ACh-binding protein is homologous to the extracellular ligand-binding domain of the ACh receptor-channel, which is thus thought to resemble this structure. The view on the left shows the ACh-binding protein in an orientation that corresponds to looking down at the ACh receptor-channel from the extracellular side of the membrane. The view on the right shows the ACh-binding protein in an orientation that corresponds to looking at the side of the extracellular portion of the ACh receptor-channel with the membrane below. (Reproduced, with permission, from Celie et al. 2004.)

B. A model for the ACh-receptor channel in the open and closed states. View looking at the side of the channel, showing two of five subunits. The structure of the extracellular region is based on the structure of the ACh-binding protein. The structure of the membrane helixes is based on electron diffraction analysis of two-dimensional crystals of the ACh receptor-channel from electric fish. The M2 helixes line the pore (see Figure 9-14B). In the closed channel (left) a hydrophobic girdle of leucine and valine residues constricts the pore, preventing ion permeation. The channel opens (right) when ACh binding induces a rotation in the extracellular binding domain that leads to a corresponding rotation in the M2 helix, widening the pore and permitting ion permeation. (Reproduced, with permission, from Unwin 2003.)

The binding of ACh to the receptor is thought to trigger a rotation of the extracellular binding domain that is somehow coupled to an opposite rotation in the M2 helixes, widening the constriction in the middle of M2 to around 0.8 to 0.9 nm, enabling ion permeation. This diameter is in reasonable agreement with electrophysiological estimates based on the pore's permeability to organic cations. The work of Karlin, however, suggests that the gate lies near the cytoplasmic mouth of the channel.

An Overall View

The terminals of motor neurons form synapses with muscle fibers at specialized regions in the muscle membrane called end-plates. When an action potential reaches the terminals of a presynaptic motor neuron it causes release of ACh. The transmitter diffuses across the synaptic cleft and binds to nicotinic ACh receptors in the end-plate, thus opening channels that allow Na^+, K^+, and Ca^{2+} to flow across the postsynaptic muscle. A net influx of Na^+ ions produces a depolarizing synaptic potential called the end-plate potential.

Because the ACh-activated channels are concentrated at the end-plate, the opening of these channels produces only a local depolarization that spreads passively along the muscle fibers. However, this local depolarization is very large. In a healthy individual it is always suprathreshold. Thus the local depolarization activates a sufficient number of voltage-gated Na^+ channels in the end-plate to generate an action potential that actively propagates along the length of the muscle.

The protein that forms the nicotinic ACh receptor-channel has been purified, its genes cloned, and its amino acids sequenced. It is composed of five subunits, two of which—the α-subunits that recognize and bind ACh—are identical. Each subunit has four hydrophobic regions that are thought to form membrane-spanning α-helixes. The protein also contains two sites for recognizing and binding ACh. This channel is thus

gated directly by a chemical transmitter. The functional molecular domains of the ACh receptor have been identified, and the steps that link ACh-binding to the opening of the channel are now being investigated. Although the atomic-level structure of the ACh receptor-channel has not been resolved, the structures of bacterial ligand-gated channels that are closely related to the ACh receptor have been resolved. Thus we may soon be able to see in atomic detail the molecular dynamics of the ACh receptor-channel's physiological functions.

The large number of ACh receptor-channels at the end-plate ensures that synaptic transmission will proceed with a high safety factor. In the autoimmune disease myasthenia gravis, antibodies to the ACh receptor decrease the number of ACh receptors, thus seriously compromising transmission at the neuromuscular junction (see Chapter 14). Certain congenital mutations in the ACh receptor subunits also contribute to a family of diseases of the neuromuscular junction termed congenital myasthenic syndrome. In some instances these mutations shorten the duration of channel opening, decreasing current during an excitatory postsynaptic potential. Other mutations prolong the opening of the ACh receptor-channels (slow channel syndrome). This leads to excessive Ca^{2+} influx, which is thought to promote degeneration of the end-plate.

Acetylcholine is only one of many neurotransmitters in the nervous system, and the end-plate potential is just one example of chemical signaling. Do transmitters in the central nervous system act in the same fashion, or are other mechanisms involved? In the past such questions were virtually unanswerable because of the small size and great variety of nerve cells in the central nervous system. However, advances in experimental technique—in particular, the patch clamp—have made synaptic transmission at central synapses easier to study. Already it is clear that many neurotransmitters operate in the central nervous system much as ACh operates at the end-plate, although other transmitters produce their effects in quite different ways. Some of the many variations of synaptic transmission that characterize the central and peripheral nervous systems are discussed in the next two chapters.

Postscript: The End-Plate Current Can Be Calculated from an Equivalent Circuit

The current through a population of ACh receptor-channels can be described by Ohm's law. However, to fully describe how the electrical current generates the end-plate potential, all the resting channels in the surrounding membrane must be considered. Because channels are proteins that span the bilayer of the membrane, we must also take into consideration the capacitive properties of the membrane and the ionic batteries determined by the distribution of Na^+, and K^+ inside and outside the cell.

The dynamic relationship of these various components can be explained using the same rules we used in Chapter 6 to analyze the current in passive electrical devices that consist only of resistors, capacitors, and batteries. We can represent the end-plate region with an equivalent circuit that has three parallel branches: (1) one representing the synaptic current through the transmitter-gated channels; (2) one representing the return current through resting channels (the non-synaptic membrane); and (3) one representing current across the lipid bilayer, which acts as a capacitor (Figure 9–16).

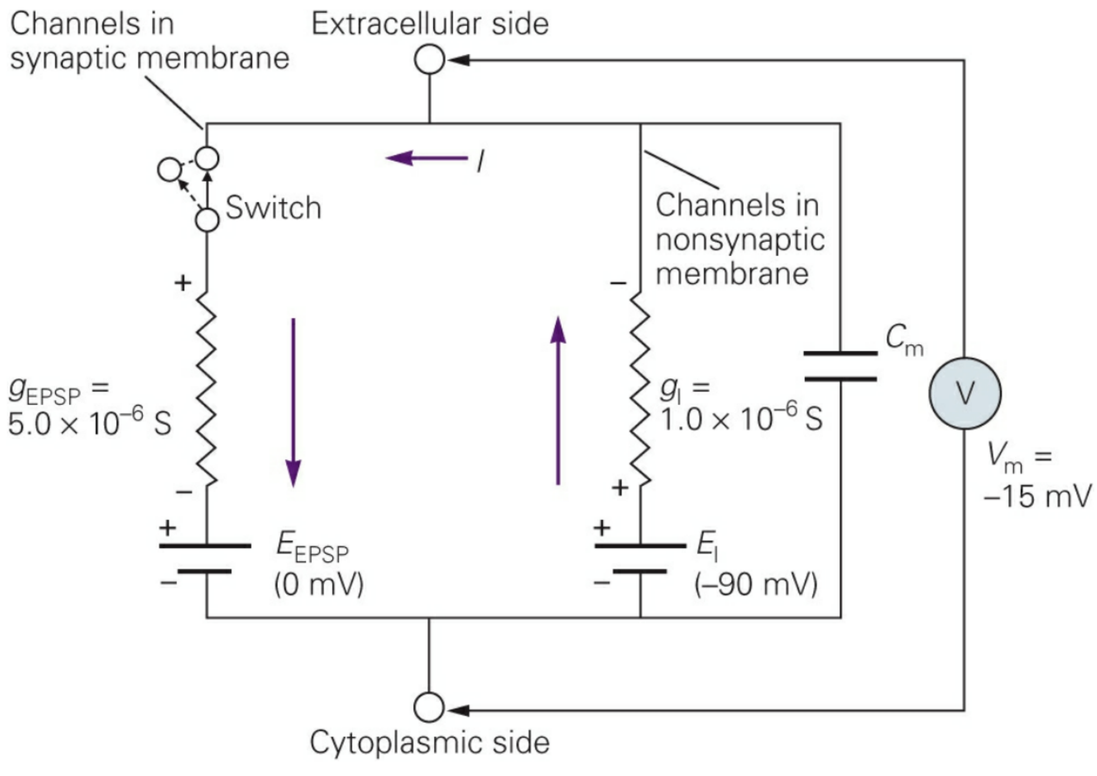

Figure 9-16 The equivalent circuit of the end-plate. The circuit has three parallel current pathways. One conductance pathway represents

the end-plate current and consists of a battery, E_{EPSP}, in series with the conductance of the ACh receptor-channels, g_{EPSP}. Another conductance pathway represents current through the nonsynaptic membrane and consists of a battery representing the resting potential (E_l) in series with the conductance of the resting channels (g_l). In parallel with both of these conductance pathways is the membrane capacitance (C_m). The voltmeter (V) measures the potential difference between the inside and the outside of the cell.

When no ACh is present, the end-plate channels are closed and carry no current. This state is depicted as an open electrical circuit in which the synaptic conductance is not connected to the rest of the circuit. The binding of ACh opens the synaptic channel. This event is electrically equivalent to throwing the switch that connects the gated conductance pathway (g_{EPSP}) with the resting pathway (g_l). In the steady state there is an inward current through the ACh-gated channels and an outward current through the resting channels. With the indicated values of conductances and batteries, the membrane will depolarize from -90 mV (its resting potential) to -15 mV (the peak of the end-plate potential).

Because the end-plate current is carried by both Na^+, and K^+, we could represent the synaptic branch of the equivalent circuit as two parallel branches, each representing the flow of a different ion species. At the end-plate, however, Na^+, and K^+ flow through the same ion channel. It is therefore more convenient (and correct) to combine the Na^+, and K^+ current pathways into a single conductance (g_{EPSP}), representing the ACh-gated channels.

The conductance of this pathway depends on the number of channels opened, which in turn depends on the concentration of transmitter. In the absence of transmitter no channels are open, and the conductance is zero. When a presynaptic action potential causes the release of transmitter, the conductance of this pathway increases to a value of approximately 5×10^{-6} S (or a resistance of 2×10^5 Ω). This is about five times the conductance of the parallel branch representing the resting or leakage channels (g_l).

The end-plate conductance is in series with a battery (E_{EPSP}), with a value given by the reversal potential for synaptic current (0 mV) (Figure 9–16). This value is the weighted algebraic sum of the Na^+, and K^+ equilibrium potentials (see Box 9-1).

The current during the excitatory postsynaptic potential (I_{EPSP}) is given by

$$I_{EPSP} = g_{EPSP} \times (V_m - E_{EPSP}).$$

Using this equation and the equivalent circuit of Figure 9-16 we can now analyze the end-plate potential in terms of ionic currents (Figure 9–17).

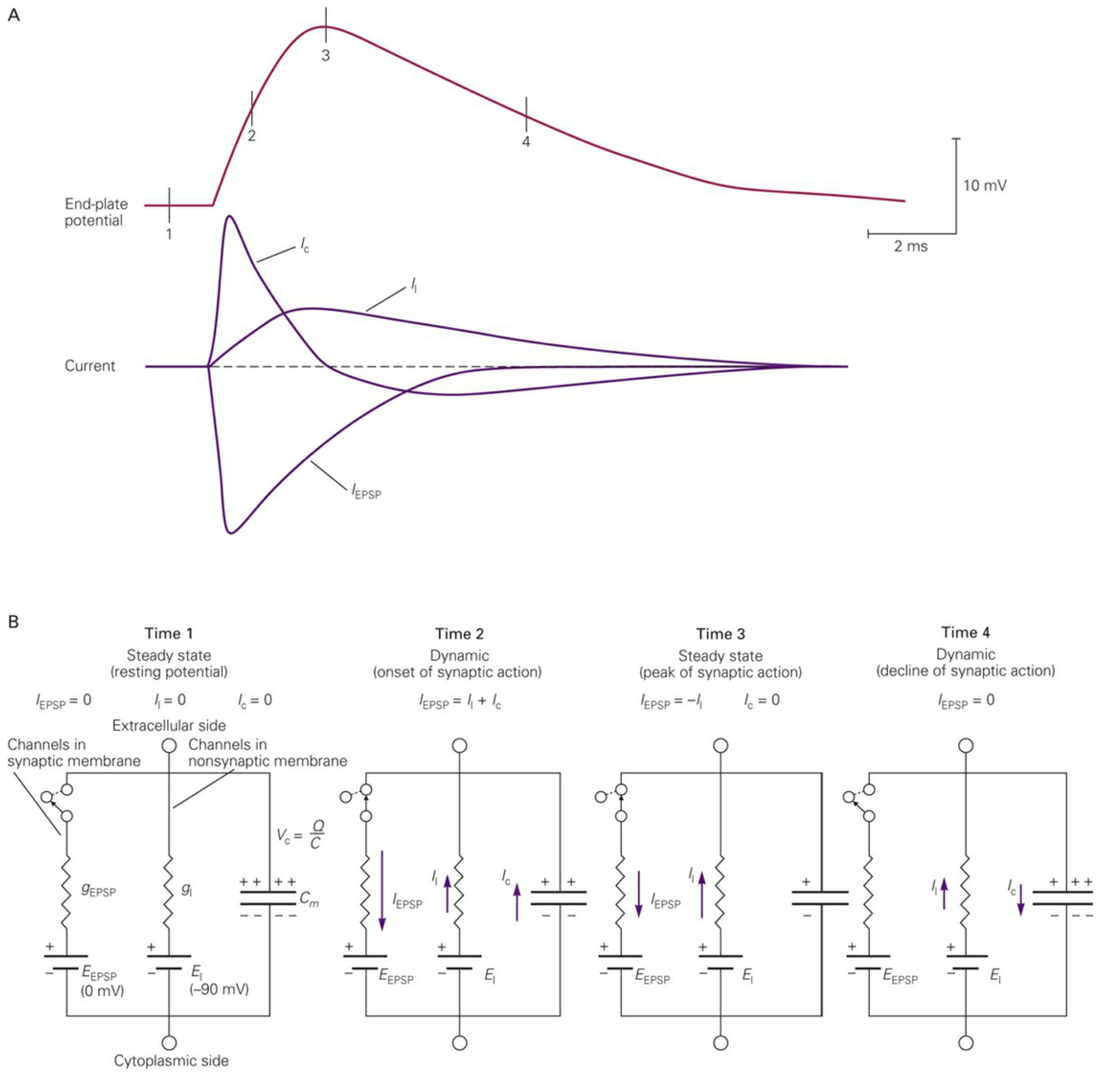

Figure 9-17 Both the ACh-gated synaptic conductance and the passive membrane properties of the muscle cell determine the time course of the end-plate potential.

A. The time course of the end-plate potential and the component currents through the ACh receptor-channels (I_{EPSP}), the resting (or leakage) channels (I_l), and the capacitor (I_c). There is a capacitive current only when the membrane potential is changing. In the steady state, such as at the peak of the end-plate potential, the inward flow of positive charge through the ACh receptor-channels is exactly balanced by the outward ionic current across the resting channels, and there is no capacitive current.

B. Equivalent circuits for the current at times 1, 2, 3, and 4 shown in part A. (The relative magnitude of a current is represented by the arrow length.)

At the onset of the excitatory synaptic action (the dynamic phase), an inward current (I_{EPSP}) is generated by the ACh-gated channels because of the increased conductance to Na^+, and K^+, and the large inward driving force on Na^+ at the resting potential of –90 mV (Figure 19–17B, time 2). Because charge must flow in a closed loop, the inward synaptic current must leave the cell as outward current. The equivalent circuit includes two parallel pathways for outward current: a conductance pathway (I_l) representing current through the resting (or leakage) channels and a capacitive pathway (I_c) representing current across the membrane capacitance. Thus,

$$I_{EPSP} = -(I_l + I_c).$$

During the earliest phase of the end-plate potential the membrane potential, V_m, is still close to its resting value, E_l. As a result, the outward driving force on current through the resting channels (V_m - E_l) is small. Therefore most of the current leaves the cell as capacitive current and the membrane depolarizes rapidly (Figure 9–17B, time 2). As the cell depolarizes, the outward driving force on current through the resting channels increases, while the inward driving force on synaptic current through the ACh receptor-channels decreases. Concomitantly, as the concentration of ACh in the synapse decreases, the ACh receptor-channels begin to close, and eventually the inward current through the gated channels is exactly balanced by outward current through the resting channels ($I_{EPSP} = -I_l$). At this point there is no current into or out of the capacitor, ($I_c = 0$). Because the rate of change of membrane potential is directly proportional to I_c,

$$I_c / C_m = \Delta V / \Delta t,$$

the membrane potential will have reached a peak or new steady-state value, $\Delta V/\Delta t = 0$ (Figure 9–17B, time 3).

As the ACh-gated channels close, I_{EPSP} decreases further. Now I_{EPSP} and I_l are no longer in balance and the membrane potential starts to repolarize, because the outward current through leak channels (I_l) becomes larger than the inward synaptic current. During most of the declining phase of the synaptic action there is no current through the ACh receptor-channels because all these channels are closed. Instead, current passes through the membrane only as outward current carried by resting channels balanced by inward current across the membrane capacitor (Figure 9–17B, time 4).

When the end-plate potential is at its peak or steady-state value, $I_c = 0$ and therefore the value of V_m can be easily calculated. The inward current through the ACh-gated channels (I_{EPSP}) must be exactly balanced by outward current through the resting channels (I_l):

$$I_{EPSP} + I_l = 0. \qquad \textbf{(9–8)}$$

The current through the ACh receptor-channels (I_{EPSP}) and resting channels (I_l) is given by Ohm's law:

$$I_{EPSP} = g_{EPSP} \times (V_m - E_{EPSP}),$$

and

$$I_l = g_l \times (V_m - E_l).$$

By substituting these two expressions into Equation 9–8, we obtain

$$g_{EPSP} \times (V_m - E_{EPSP}) + g_l \times (V_m - E_l) = 0.$$

To solve for V_m we need only expand the two products in the equation and rearrange them so that all terms in voltage appear on the left side:

$$(g_{EPSP} \times V_m) + (g_l \times V_m) = (g_{EPSP} \times E_{EPSP}) + (g_l \times E_l).$$

By factoring out V_m on the left side, we finally obtain

$$V_m = \frac{(g_{EPSP} \times E_{EPSP}) + (g_l \times E_l)}{g_{EPSP} + g_l}. \qquad \textbf{(9–9)}$$

This equation is similar to that used to calculate the resting and action potentials (see Chapter 6). According to Equation 9–9, the peak voltage of the end-plate potential is a weighted average of the electromotive forces of the two batteries for ACh-gated and resting currents. The weighting factors are given by the relative magnitude of the two conductances. If

the ACh-gated conductance is much smaller than the resting conductance ($g_{EPSP} \ll g_l$), $g_{EPSP} \times E_{EPSP}$ will be negligible compared with $g_l \times E_l$. Under these conditions V_m will remain close to E_l. This situation occurs when only a few ACh receptor-channels are opened, because the ACh concentration is low. Conversely, if g_{EPSP} is much larger than g_l, Equation 9–9 states that V_m approaches E_{EPSP}, the synaptic reversal potential. This situation occurs when a large number of ACh-activated channels are open, because the concentration of ACh is high. At intermediate ACh concentrations, with a moderate number of ACh-activated channels open, the peak end-plate potential lies somewhere between E_l and E_{EPSP}.

We can now calculate the peak end-plate potential for the specific case shown in Figure 9-16, where $g_{EPSP} = 5 \times 10^{-6}$ S, $g_l = 1 \times 10^{-6}$ S, $E_{EPSP} = 0$ mV, and $E_l = -90$ mV. Substituting these values into Equation 9–9 yields

$$V_m = \frac{[(5 \times 10^{-6}\ \text{S}) \times (0\ \text{mV})] + [(1 \times 10^{-6}\ \text{S}) \times (-90\ \text{mV})]}{(5 \times 10^{-6}\ \text{S}) + (1 \times 10^{-6}\ \text{S})}.$$

or

$$V_m = \frac{(1 \times 10^{-6}\ \text{S}) \times (-90\ \text{mV})}{(6 \times 10^{-6}\ \text{S})}$$

$$= -15\ \text{mV}.$$

The peak amplitude of the end-plate potential is then

$$\Delta V_{EPSP} = V_m - E_l = -15\ \text{mV} - (-90\ \text{mV}) = 75\ \text{mV}.$$

As a check for consistency we can see whether, at the peak of the end-plate potential, the synaptic current is equal and opposite to the nonsynaptic current so that the net membrane current is indeed equal to zero:

$$I_{EPSP} = (5 \times 10^{-6}\ \text{S}) \times (-15\ \text{mV} - 0\ \text{mV}) = -75 \times 10^{-9}\ \text{A}$$

and

$$I_l = (1 \times 10^{-6}\ \text{S}) \times [-15\ \text{mV} - (-90\ \text{mV})] = 75 \times 10^{-9}\ \text{A}.$$

Here we see that Equation 9–9 ensures that $I_{EPSP} + I_l = 0$.

Eric R. Kandel
Steven A. Siegelbaum

Selected Readings

Changeux JP. 2010. Allosteric receptors: from electric organ to cognition. Annu Rev Pharmacol Toxicol 50:1–38.

Fatt P, Katz B. 1951. An analysis of the end-plate potential recorded with an intracellular electrode. J Physiol 115:320–370.

Heuser JE, Reese TS. 1977. Structure of the synapse. In: ER Kandel (ed). *Handbook of Physiology: A Critical, Comprehensive Presentation of Physiological Knowledge and Concepts*, Sect. 1 *The Nervous System*, Vol. 1 *Cellular Biology of Neurons*, Part 1, pp. 261–294. Bethesda, MD: American Physiological Society.

Hille B. 2001. *Ion Channels of Excitable Membranes*, 3rd ed., pp. 169–199. Sunderland, MA: Sinauer.

Imoto K, Busch C, Sakmann B, Mishina M, Konno T, Nakai J, Bujo H, Mori Y, Fukuda K, Numa S. 1988. Rings of negatively charged amino acids determine the acetylcholine receptor-channel conductance. Nature 335:645–648.

Karlin A. 2002. Emerging structure of the nicotinic acetylcho-line receptors. Nat Rev Neurosci 3:102–114.

Neher E, Sakmann B. 1976. Single-channel currents recorded from membrane of denervated frog muscle fibres. Nature 260:799–802.

Unwin N. 2005. Refined structure of the nicotinic acetylcholine receptor at 4 Å resolution. J Mol Biol 346:967–989.

References

Akabas MH, Kaufmann C, Archdeacon P, Karlin A. 1994. Identification of acetylcholine receptor-channel lining residues in the entire M2 segment of the α-subunit. Neuron 13:919–927.

Alberts B, Bray D, Lewis J, Raff M, Roberts K, Watson JD. 1989. *Molecular Biology of the Cell*, 2nd ed. New York: Garland.

Brejc K, van Dijk WJ, Klaassen RV, Schuurmans M, van der Oost J, Smit AB, Sixma TK. 2001. Crystal structure of an ACh-binding protein reveals the ligand-binding domain of nicotinic receptors. Nature 411:269–276.

Brisson A, Unwin PN. 1985. Quaternary structure of the acetylcholine receptor. Nature 315:474–477.

Celie PH, van Rossum-Fikkert SE, van Dijk WJ, Brejc K, Smit AB, Sixma TK. 2004. Nicotine and carbamylcholine binding to nicotinic acetylcholine receptors as studied in AChBP crystal structures. Neuron 41:907–914.

Charnet P, Labarca C, Leonard RJ, Vogelaar NJ, Czyzyk L, Gouin A, Davidson N, Lester HA. 1990. An open channel blocker interacts with adjacent turns of α-helices in the nicotinic acetylcholine receptor. Neuron 4:87–95.

Claudio T, Ballivet M, Patrick J, Heinemann S. 1983. Nucleotide and deduced amino acid sequences of Torpedo californica acetylcholine receptor γ-subunit. Proc Natl Acad Sci USA 80:1111–1115.

Colquhoun D. 1981. How fast do drugs work? Trends Pharmacol Sci 2:212–217.

Dwyer TM, Adams DJ, Hille B. 1980. The permeability of the endplate channel to organic cations in frog muscle. J Gen Physiol 75:469–492.

Fertuck HC, Salpeter MM. 1974. Localization of acetylcholine receptor by 125I-labeled α-bungarotoxin binding at mouse motor endplates. Proc Natl Acad Sci USA 71:1376–1378.

Heuser JE, Salpeter SR. 1979. Organization of acetylcholine receptors in quick-frozen, deep-etched, and rotary-replicated Torpedo postsynaptic membrane. J Cell Biol 82: 150–173.

Ko C-P. 1984. Regeneration of the active zone at the frog neuromuscular junction. J Cell Biol 98:1685–1695.

Kuffler SW, Nicholls JG, Martin AR. 1984. *From Neuron to Brain: A Cellular Approach to the Function of the Nervous System*, 2nd ed. Sunderland, MA: Sinauer.

McMahan UJ, Kuffler SW. 1971. Visual identification of synaptic boutons on living ganglion cells and of varicosities in postganglionic axons in the heart of the frog. Proc R Soc Lond B Biol Sci 177:485–508.

Miles FA. 1969. *Excitable Cells*. London: Heinemann.

Miyazawa A, Fujiyoshi Y, Stowell M, Unwin N. 1999. Nicotinic acetylcholine receptor at 4.6 å resolution: transverse tunnels in the channel wall. J Mol Biol 288:765–786.

Miyazawa A, Fujiyoshi Y, Unwin N. 2003. Structure and gating mechanism of the acetylcholine receptor pore. Nature 424:949–955.

Noda M, Furutani Y, Takahashi H, Toyosato M, Tanabe T, Shimizu S, Kikyotani S, et al. 1983. Cloning and sequence analysis of calf cDNA and human genomic DNA encoding α-subunit precursor of muscle acetylcholine receptor. Nature 305:818–823.

Noda M, Takahashi H, Tanabe T, Toyosato M, Kikyotani S, Furutani Y, Hirose T, et al. 1983. Structural homology of Torpedo californica acetylcholine receptor subunits. Nature 302:528–532.

Palay SL. 1958. The morphology of synapses in the central nervous system. Exp Cell Res 5:275–293. Suppl.

Raftery MA, Hunkapiller MW, Strader CD, Hood LE. 1980. Acetylcholine receptor: complex of homologous subunits. Science 208:1454–1457.

Revah F, Galzi J-L, Giraudat J, Haumont PY, Lederer F, Changeux J-P. 1990. The noncompetitive blocker [3H] chlorpromazine labels three amino acids of the acetylcholine receptor gamma subunit: implications for the alpha-helical organization of regions MII and for the structure of the ion channel. Proc Natl Acad Sci USA 87:4675–4679.

Salpeter MM (ed). 1987. *The Vertebrate Neuromuscular Junction*, pp. 1–54. New York: Liss.

Takeuchi A. 1977. Junctional transmission. I. Postsynaptic mechanisms. In: ER Kandel (ed). *Handbook of Physiology: A Critical, Comprehensive Presentation of Physiological Knowledge and Concepts*, Sect. 1 *The Nervous System*, Vol. 1 *Cellular Biology of Neurons*, Part 1, pp. 295–327. Bethesda, MD: American Physiological Society.

Toyoshima C, Unwin N. 1988. Ion channel of acetylcholine receptor reconstructed from images of postsynaptic membranes. Nature 336:247–250.

Verrall S, Hall ZW. 1992. The N-terminal domains of acetylcholine receptor subunits contain recognition signals for the initial steps of receptor assembly. Cell 68:23–31.

Villarroel A, Herlitze S, Koenen M, Sakmann B. 1991. Location of a threonine residue in the alpha-subunit M2 transmembrane segment that determines the ion flow through the acetylcholine receptor-channel. Proc R Soc Lond B Biol Sci 243:69–74.

Unwin N. 1995. Acetylcholine receptor-channel imaged in the open state. Nature 373:37–43.

Unwin N. 2003. Structure and action of the nicotinic acetylcholine receptor explored by electron microscopy. FEBS Lett 555:91–95.